Pentraxin 3 deletion aggravates allergic inflammation through a T_H17-dominant phenotype and enhanced CD4 T-cell survival

Jyoti Balhara, MSc,[a] Lianyu Shan, MSc,[a] Jingbo Zhang, PhD,[a]* Anik Muhuri, BSc,[a] Andrew J. Halayko, PhD,[b] Muhamad S. Almiski, MD,[c] Diana Doeing, MD,[d] John McConville, MD,[d] Martin M. Matzuk, MD, PhD,[e] and Abdelilah S. Gounni, PhD[a] *Winnipeg, Manitoba, Canada; Chicago, Ill; and Houston, Tex*

GRAPHICAL ABSTRACT

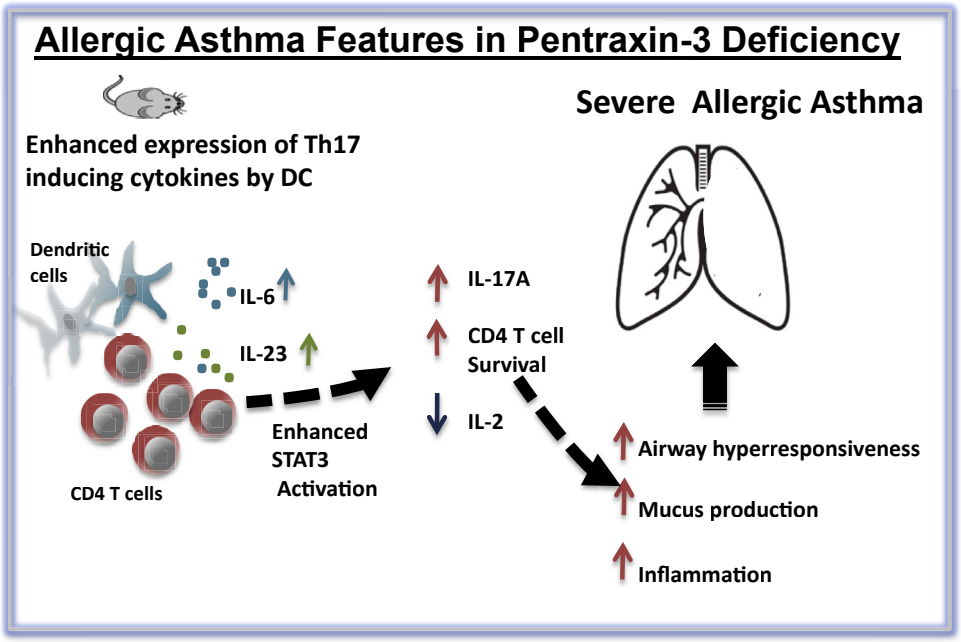

Background: Pentraxin 3 (PTX3) is a multifunctional molecule that plays a nonredundant role at the crossroads between pathogen clearance, innate immune system, matrix deposition, female fertility, and vascular biology. It is produced at sites of infection and inflammation by both structural and inflammatory cells. However, its role in allergen-induced inflammation remains to be tested.

Objective: We sought to determine the effect of *Ptx3* deletion on ovalbumin (OVA)–induced allergic inflammation in a murine model of asthma.

Methods: Bronchoalveolar lavage fluid was collected from patients with severe asthma and healthy subjects, and the level of PTX3 was determined by using ELISA. *Ptx3*$^{+/+}$ and *Ptx3*$^{-/-}$ mice were sensitized and challenged with OVA and bronchoalveolar lavage fluid, and the lungs were collected for assessing inflammation. Lung tissue inflammation and mucus production were assessed by means of flow cytometry and hematoxylin and eosin and periodic acid-Schiff staining, respectively. flexiVent was used to determine airway resistance to methacholine in these mice.

Results: Here we report that mice with severe asthma and OVA-sensitized/challenged mice had increased PTX3 levels in the lungs compared with healthy control mice. Mice lacking PTX3 have exaggerated neutrophilic/eosinophilic lung inflammation, mucus production, and airway hyperresponsiveness in an experimental model of OVA-induced

From the Departments of [a]Immunology, [b]Physiology, and [c]Pathology, Max Rady College of Medicine, Rady Faculty of Health Sciences, University of Manitoba, Winnipeg; [d]the Department of Medicine, University of Chicago; and [e]the Department of Pathology & Immunology, Baylor College of Medicine, Houston.

*Dr Zhang is currently affiliated with the Department of Nephrology, Third Military University Hospital, Chongqing, China.

Support for this work was provided by the Children's Hospital Research Institute of Manitoba and Manitoba Health Research Council Research Chair (to A.S.G.), the Children's Hospital Research Institute of Manitoba postdoctoral award (to J.Z.), and the Canadian Institute of Health Research (CIHR; grant no. 115115 to A.S.G.). *Ptx3*$^{-/-}$ mice were created with the support of the Eunice Kennedy Shriver National Institute of Child Health and Human grant HD033438.

Disclosure of potential conflict of interest: The authors declare that they have no relevant conflicts of interest.

Received for publication April 22, 2015; revised April 1, 2016; accepted for publication April 28, 2016.

Corresponding author: Abdelilah S. Gounni, PhD, Department of Immunology, College of Medicine, Faculty of Health Sciences, University of Manitoba, 419 Apotex Centre, 750 McDermot Ave, Winnipeg, Manitoba R3E 0T5, Canada. E-mail: abdel.gounni@umanitoba.sca.

0091-6749/$36.00

© 2016 American Academy of Allergy, Asthma & Immunology

http://dx.doi.org/10.1016/j.jaci.2016.04.063

asthma. Furthermore, OVA-exposed lung *Ptx3*$^{-/-}$ CD4 T cells exhibit an increased production of IL-17A, an effect that is accompanied by an increased signal transducer and activator of transcription 3 phosphorylation, reduced IL-2 production, and enhanced activation and survival. Also, we observed an increase in numbers of IL-6– and IL-23–producing dendritic cells in OVA-exposed *Ptx3*$^{-/-}$ mice compared with those in wild-type control mice.

Conclusion: Altogether, PTX3 deficiency results in augmented airway hyperresponsiveness, mucus production, and IL-17A–dominant pulmonary inflammation, suggesting a regulatory role of PTX3 in the development of allergic inflammation. (J Allergy Clin Immunol 2016;■■■:■■■-■■■.)

Key words: *Pentraxin 3, allergic inflammation, CD4 T cells, IL-17A, IL-2, survival, B-cell lymphoma 2, signal transducer and activator of transcription 3, dendritic cells, IL-6*

Abbreviations used

AHR:	Airway hyperresponsiveness
BALF:	Bronchoalveolar lavage fluid
Bcl-2:	B-cell lymphoma 2
CFSE:	Carboxyfluorescein succinimidyl ester
DC:	Dendritic cell
H&E:	Hematoxylin and eosin
MCh:	Methacholine
MLN:	Mediastinal lymph node
OVA:	Ovalbumin
PAS:	Periodic acid-Schiff
PRR:	Pattern recognition receptor
PTX3:	Pentraxin 3
SARS:	Severe acute respiratory syndrome
SNP:	Single nucleotide polymorphism
STAT3:	Signal transducer and activator of transcription 3

According to the World Health Organization, asthma is a serious public health concern affecting more than 300 million persons worldwide. Furthermore, the disease prevalence globally increases by approximately 50% every decade.[1] According to Braman,[1] a collateral increase in atopic sensitization and other allergic conditions, such as eczema and rhinitis, is associated with an increase in asthma pervasiveness. Genetic predisposition,[2,3] environmental factors,[4] and gene-environment interactions contribute to the increased asthma prevalence in susceptible subjects.

Asthma is classically defined as a disease orchestrated by the adaptive immune system. However, recent advances suggest considerable crosstalk between the innate and adaptive immune systems in initiation and propagation of allergic immune response.[5] Pattern recognition receptors (PRRs), such as Toll-like receptors, are key components of the innate immune system that have been found to play an important role in allergic inflammation. PRRs on epithelial cells and dendritic cells (DCs) recognize pathogen-associated molecular patterns and damage-associated molecular patterns and act as adjuvants in directing allergen sensitization.[6-8]

Pentraxin 3 (PTX3) is a prototypic soluble PRR involved in the regulation of inflammation through multiple mechanisms that include interaction with components of complement pathways, Fcγ receptors, pathogenic moieties on microbes, and regulation of leukocyte migration.[9] Previously, lack of PTX3 has been reported to exaggerate inflammation in the setting of *Pseudomonas aeruginosa* infection, aspergillosis, influenza, severe acute respiratory syndrome (SARS), and LPS-induced acute lung injury in mice. The protective role of exogenous PTX3 in aspergillosis, pneumonia, and tuberculosis further strengthens the preceding observations (reviewed by Balhara et al[9]). Collectively, these studies demonstrate that infection and lung injury increase PTX3 production in the lung.[9]

Previously published data by our group[10] showed enhanced PTX3 expression in the lungs of patients with severe allergic asthma compared with that in healthy donors. Structural cells, particularly epithelial and airway smooth muscle cells, were the main producers of PTX3 *in vivo* and on proinflammatory cytokine stimulation *in vitro*. However, the role of PTX3 in the development of allergic asthma remains unknown.

In this study our aim is to evaluate the effect of PTX3 deletion in the development of ovalbumin (OVA)–induced physiologic and immunologic metrics. Here we show that deletion of PTX3 resulted in exaggerated inflammation, airway hyperresponsiveness (AHR), and airway remodeling. We also demonstrate that *Ptx3*$^{-/-}$ mice exhibit a T_H17-dominant inflammatory response compared with *Ptx3*$^{+/+}$ mice in response to OVA. Altogether, our report suggests a critical role of PTX3 in regulating CD4 T cell–mediated inflammation in a murine model of allergen-induced inflammation.

METHODS

Subjects

Bronchoalveolar lavage fluid (BALF) used in this study was obtained from nonasthmatic healthy subjects and patients with severe asthma in accordance with procedures approved by the Human Research Ethics Board of the University of Chicago (Institutional Review Board nos. 13198A and 15361A). All subjects were seen in a refractory obstructive lung disease clinic by an asthma/chronic obstructive pulmonary disease expert. Subjects were consented at the time of preoperative clinic visits. Pulmonary function tests were performed with methacholine (MCh) challenge before surgery. All surgeries were elective and for noninfectious or noninflammatory reasons: most of the surgeries were performed on obese patients and were bariatric in nature. One of the surgeries was for a thyroid nodule. Most of the donors showed no symptoms of comorbidities, except asthmatic patient 4, who was given a diagnosis of kyphoscoliosis. All bronchoscopies were done for research purposes only. Detailed clinical characteristics of the donors have been provided in Tables I and II. Details of healthy control subjects are provided in Table III. BALF was concentrated 10 times with Ultracel 10K cutoff concentrating centrifugal filter units (Millipore, Temecula, Calif).

Animals

Female *Ptx3*$^{-/-}$ and *Ptx3*$^{+/+}$ (129SvEv/Bl/6 background, 5-8 weeks old) mice were obtained from Dr M. Matzuk, Baylor College of Medicine, and bred at the University of Manitoba breeding facility. Animals were used according to the guidelines issued by the Canadian Council on Animal Care and the University of Manitoba Animal Ethics Board.

Lung mechanics

AHR to MCh was assessed, as described previously,[11] by using a flexiVent small-animal ventilator (SCIREQ, Montreal, Quebec, Canada; see the Methods section in this article's Online Repository at www.jacionline.org).

TABLE I. Clinical characteristics of donors with severe asthma subjected to BALF collection

Subjects	Age (y)	Sex	Asthma severity	Asthma duration (y)	FEV_1 (%)	FEV_1 (L)	Total IgE (IU/mL)	Smoking (pack years)	BMI (kg/m^2)	Allergens (serum)
Asthmatic patient 1	27	Female	Severe	24	50	1.45	1131	0	36.6	*Felis catus (domesticus)*, *Canis familiaris*, *Aspergillus fumigatus*, *Candida albicans*, *Stenopstesis alternata*, ragweed
Asthmatic patient 2	51	Female	Severe	9	60	1.61	146	5	53.6	Negative
Asthmatic patient 3	73	Female	Severe	57	38	0.68	368	0	NA	*Canis familiaris*, *Aspergillus fumigatus*, house dust mite
Asthmatic patient 4	47	Female	Severe	46	42	1.05	66.9	0	27.6	*Felis catus (domesticus)*, *Canis familiaris*
Asthmatic patient 5	74	Male	Severe	72	25	0.66	299	10	NA	*Stemphylium herbarum*, *Phoma betae*, *Epicoccum purpurascens*, *Trichophyton rubrum*, *Botrytis cinerea*, *Setosphaeria rostrata*, *Fusarium proliferatum*
Asthmatic patient 6	70	Female	Severe	7	50	1.18	881	0	NA	Negative
Asthmatic patient 7	74	Female	Severe	70	59	1.07	25.7	0	NA	Negative
Asthmatic patient 8	64	Female	Severe	14	41	0.81	87	0	NA	Negative
Asthmatic patient 9	47	Female	Severe	40	96	2.23	46.9	0	NA	Negative

Asthma was categorized as severe based on typical criteria by using American Thoracic Society guidelines. These subjects required treatment with high-dose inhaled corticosteroids plus a second controller (and/or systemic corticosteroids) to prevent the disease from becoming "uncontrolled" or for disease that remains "uncontrolled" despite this therapy.
BMI, Body mass index; *NA*, not available.

TABLE II. Medications of asthmatic patients

Subjects	Steroid 1 (2 times daily)	BDP equivalent/ dose/steroid 1	Other steroids	Other asthma medications
Asthmatic patient 1	1P Advair 500/50	1000 μg	10 mg of Prednisone daily	Singulair, albuterol
Asthmatic patient 2	1P Advair 500/50	1000 μg	10 mg of Prednisone daily	Singulair, Spiriva, Duoneb, albuterol
Asthmatic patient 3	1P Advair 500/50	1000 μg	10 mg of Prednisone daily plus nebulized budesonide, 1 mg/2l 2 times daily	Combivent
Asthmatic patient 4	1P Advair 500/50	1000 μg		Singulair, albuterol
Asthmatic patient 5	1P Advair 250/50	500 μg		Singulair, Spiriva, albuterol
Asthmatic patient 6	1P Advair 250/50	500 μg		Albuterol
Asthmatic patient 7	2P Symbicort 160/4.5	400 μg		Singulair, albuterol
Asthmatic patient 8	1P fluticasone 220	440 μg		Salmeterol 50, Maxair
Asthmatic patient 9	1P Advair 500/50	1000 μg		Singulair, theophylline, omalizumab, albuterol

Advair (GlaxoSmithKline, Research Triangle Park, NC): fluticasone/salmeterol; Symbicort (AstraZeneca, London, United Kingdom): budesonide/formoterol.
BDP, Beclomethasone dipropionate; *P*, puffs.

Histology

For histologic analysis, lungs were harvested and fixed in 10% buffered formalin. Tissues were then embedded in paraffin. Six-micrometer sections were cut with a microtome and stained with hematoxylin and eosin (H&E) and periodic acid-Schiff (PAS). For analysis of inflammation and mucus production, H&E and PAS staining, respectively, of lung tissues was determined under a light microscope. Two independent persons scored the slides in a blinded manner.

ELISA

PTX3 levels were determined by means of ELISA with antibodies from R&D Systems (Minneapolis, Minn). Cytokines in the lung homogenate and supernatant of *in vitro*–cultured mediastinal lymph node (MLN) cells were assayed by using ELISA MAX Deluxe sets from BioLegend (San Diego, Calif), according to the manufacturer's protocol. Immunoglobulin ELISA was performed with antibodies from SouthernBiotech (Birmingham, Ala). For more details on tissue isolation, refer to the Methods section in this article's Online Repository.

Flow cytometry

Single cells were collected from lungs and MLNs, washed with flow buffer, blocked with Fc blocker, and stained with respective antibody in the dark. Labeled cells were then acquired on a FACSCanto II (BD Biosciences, San Jose, Calif). For intracellular staining, cells were stimulated with cell stimulation cocktail (eBioscience, San Diego, Calif) for 4 hours and then stained for extracellular and intracellular markers. A detailed list of antibodies used is provided in Table E1 in this article's Online Repository at www.jacionline.org.

TABLE III. Clinical characteristics of healthy donors subjected to BALF collection

Subjects	Age (y)	Sex	FEV_1 (%)	FEV_1 (L)	PC_{20} (mg of MCh/mL)	Smoking (pack years)	Medication	Allergens (serum)
Healthy subject 1	41	Male	95	4.10	Negative	0	None	Negative
Healthy subject 2	53	Female	102	2.50	Negative	0	None	Negative
Healthy subject 3	42	Female	96	3.22	Negative	0	None	Negative
Healthy subject 5	31	Female	92	2.67	Negative	0	None	Negative
Healthy subject 6	34	Female	93	2.78	Negative	0	None	Negative
Healthy subject 8*	49	Male	69	2.35	Negative	0	None	Negative
Healthy subject 7	56	Male	72	2.34	0.22	0	None	Negative

BMI, Body mass index.
*Donor had a normal FEV_1/forced vital capacity ratio and diffusing capacity of lung for carbon monoxide value. There was no difference between total lung capacity, as calculated by using plethysmography and the single-breath method, which suggests the absence of any obstruction.

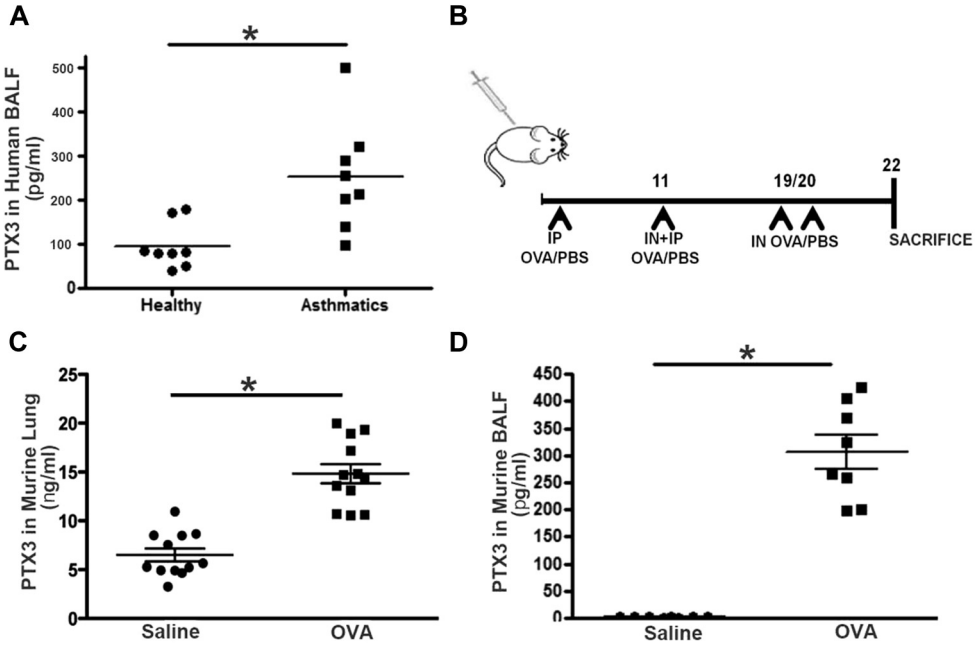

FIG 1. A, PTX3 concentrations are increased in the setting of asthma in human subjects and mice. PTX3 levels in BALF obtained from healthy subjects and patients with severe asthma were evaluated by means of ELISA. $*P < .01$. **B,** Schematic showing the protocol used for acute OVA sensitization/challenge in mice. *IN*, Intranasal; *IP*, intraperitoneal. **C** and **D,** PTX3 concentrations measured in the lungs (Fig 1, *C*) and BALF (Fig 1, *D*) of $Ptx3^{+/+}$ mice in saline- and OVA-exposed conditions. $*P < .01$.

Statistical analysis

Results are shown as means ± SEMs and analyzed by using 1-way ANOVA (GraphPad Prism; GraphPad Software, La Jolla, Calif). For experiments in which only 2 data sets are compared, the Student *t* test or Wilcoxon signed-rank test was performed. Unless otherwise stated, data were collected from at least 3 experiments, with each experiment containing at least 3 to 5 mice in each experimental group. A *P* value of less than .05 was considered significant in all quantitative experiments.

RESULTS

PTX3 levels are enhanced in human asthma

PTX3 expression has been shown to be increased in patients with several pulmonary diseases, including cigarette smoke–induced chronic obstructive pulmonary disease, LPS-induced acute lung injury, and murine SARS infection.[9] Previously, we have shown augmented expression of PTX3 in bronchial biopsy specimens obtained from patients with severe allergic asthma compared with healthy subjects.[10] We further validated this in BALF of human patients with severe asthma compared with healthy donors (Tables I-III). Patients with severe asthma exhibit greater concentrations of PTX3 in BALF compared with healthy donors (240.2 ± 58.6 vs 78.60 ± 47.6 pg/mL; n = 10; $P < .01$; Fig 1, *A*).

PTX3 concentrations are increased in OVA-exposed murine lungs

Next, we sought to determine PTX3 production in the lungs of mice in response to acute OVA exposure. Mice were sensitized with OVA plus alum intraperitoneally on days 1 and 11 and challenged intranasally on days 18 and 19 (Fig 1, *B*). OVA-sensitized and challenged mice display a significant increase in BALF and lung PTX3 concentrations compared with their saline controls (BALF PTX3: 321 ± 89 vs 9.36 ± 1.06 pg/mL; lung PTX3: 14.8 ± 1.4 vs 6.1 ± 0.8 ng/mL; n = 8-12; $P < .01$; Fig 1, *C*).

Deletion of PTX3 exacerbates allergic inflammation in mice

Given that PTX3 levels increase in the setting of asthma and that $Ptx3^{-/-}$ mice exhibit enhanced susceptibility to various

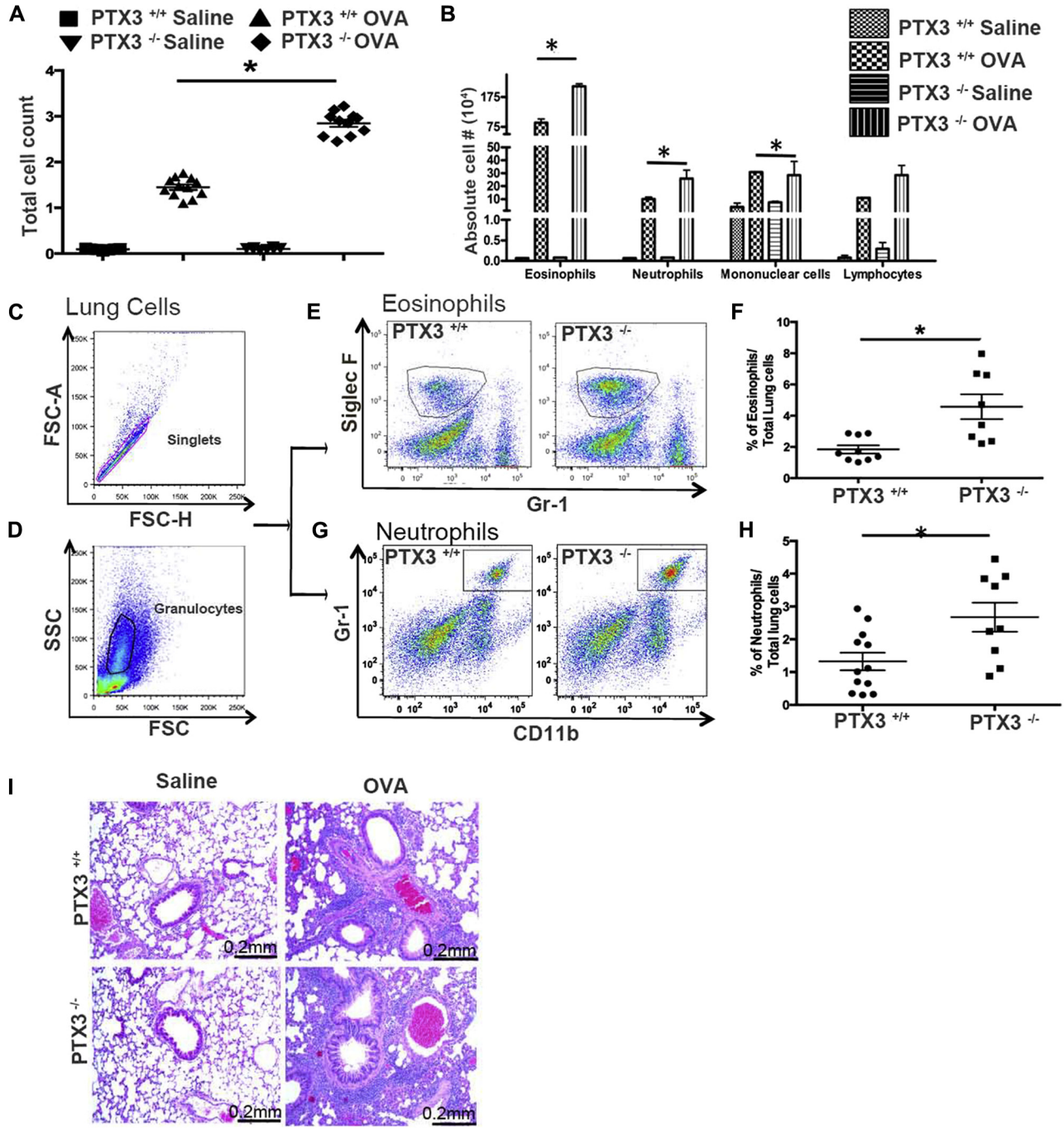

FIG 2. Disruption of PTX3 worsens airway and lung inflammation. **A** and **B,** Total (Fig 2, *A*) and differential (Fig 2, *B*) cell counts in BALF of OVA-sensitized/challenged and saline-exposed *Ptx3*$^{+/+}$ and *Ptx3*$^{-/-}$ mice. **C-H,** Flow cytometric analysis of singlets (Fig 2, *C*) and granulocytes (Fig 2, *D*): eosinophils (Fig 2, *E* and *F*) and neutrophils (Fig 2, *G* and *H*) in the lungs of mice from both strains 48 hours after OVA challenge (n = 8-9 per group). *$P < .01$. *FSC*, Forward scatter; *SSC*, side scatter. **I,** Histologic examination of lung inflammation (×200 magnification).

infections (reviewed by Balhara et al[9]), we sought to examine the consequences of PTX3 deletion on airway inflammatory response in an OVA-induced murine model of experimental asthma. We first determined influx of inflammatory cells in the airway lumen. There was a significant infiltration of inflammatory cells into the airways of *Ptx3*$^{+/+}$ and *Ptx3*$^{-/-}$ mice after OVA challenge; however, *Ptx3*$^{-/-}$ mice exhibited a greater number of total inflammatory cells (n = 12; $P < .01$; Fig 2, *A*, and Table IV). Although both genotypes showed an eosinophil-dominant response on OVA challenge, *Ptx3*$^{-/-}$ mice exhibited greater BALF eosinophil counts (Fig 2, *B*, and Table IV) and lung tissue eosinophilia (Siglec F^{high}/Gr-1$^{low/-}$; Fig 2, *E* and *F*) compared with their *Ptx3*$^{+/+}$ counterparts. Greater neutrophil counts in the airways and lungs (CD11b^{+}/Gr-1^{+}) were also detected in

TABLE IV. Summary of infiltrating inflammatory cells in airways and lung tissues of OVA-challenged/sensitized *Ptx3*$^{+/+}$ and *Ptx3*$^{-/-}$ mice

Cell types	*Ptx3*$^{+/+}$ OVA	*Ptx3*$^{-/-}$ OVA
Total cells (airways)	$1.6 \times 10^6 \pm 2840$	$2.9 \times 10^6 \pm 4100$†
Eosinophils (airways)	$79.3 \times 10^4 \pm 2300$	$177.6 \times 10^4 \pm 4603$†
Neutrophils (airways)	$8.7 \times 10^4 \pm 820$	$24 \times 10^4 \pm 1460$†
Eosinophils (lungs)*	1.8% ± 0.3%	4.6% ± 0.8%†
Neutrophils (lungs)*	1.3% ± 0.26%	2.6% ± 0.44%†

*Percentage of total lung cells.
†$P < .05$.

Ptx3$^{-/-}$ mice compared with their P*tx*3$^{+/+}$ counterparts (Fig 2, *B*, *G*, and *H*, respectively).[12] Enhanced infiltration of inflammatory cells surrounding the airways and blood vessels in *Ptx3*$^{-/-}$ mice compared with *Ptx3*$^{+/+}$ mice was further supported by an examination of H&E-stained lung sections (Fig 2, *I*).

OVA sensitization and subsequent challenge are known to affect immunoglobulin concentrations in blood.[13,14] Indeed, serum levels of total (Fig 3, *A* and *C*) and OVA-specific (Fig 3, *B* and *D*) IgE and IgG_{2a} were substantially increased in *Ptx3*$^{-/-}$ mice compared with *Ptx3*$^{+/+}$ mice. Taken together, our data indicate that lack of PTX3 results in an enhanced recruitment of granulocytes, particularly eosinophils and neutrophils, and IgE/IgG_{2a} secretion.

Ptx3$^{-/-}$ mice display enhanced AHR and airway remodeling

As a measure of altered lung mechanics in response to allergen, we determined the response of *Ptx3*$^{-/-}$ and *Ptx3*$^{+/+}$ mice to MCh after allergen (OVA) exposure. OVA challenge resulted in amplified AHR, as determined by measuring airway resistance to inhaled MCh in *Ptx3*$^{-/-}$ mice (n = 12; $P < .01$; Fig 4, *A*) compared with *Ptx3*$^{+/+}$ mice. We also observed evidence of enhanced goblet cell hyperplasia, as determined by using PAS staining (Fig 4, *B* and *C*), and expression of *muc5ac* (Fig 4, *D*) and *muc5b (*Fig 4, *E)* in *Ptx3*$^{-/-}$ mice in contrast to *Ptx3*$^{+/+}$ mice. These results collectively indicate that PTX3 deletion aggravates OVA-induced AHR and mucus production.

Ptx3$^{-/-}$ mice exhibit enhanced IL-17A levels in the lungs and MLNs

Evaluation of cytokine production in the lungs and MLNs is an essential parameter used to assess allergic inflammation.[15,16] Therefore we next explored the levels of IL-4, IFN-γ, and IL-17A in lung homogenates and MLNs. OVA exposure induced T_H2 response, as determined by IL-4 (Fig 5, *A*) and IL-5 (see Fig E1, *D*, in this article's Online Repository at www.jacionline.org) levels in the lungs of both strains of mice compared with their saline-exposed counterparts. Absolute concentrations of IL-4 (*Ptx3*$^{-/-}$: 25.1 ± 2.5 pg/mL vs *Ptx3*$^{+/+}$: 52.9 ± 3.9 pg/mL) and IL-5 (*Ptx3*$^{-/-}$: 122.8 ± 47 pg/mL vs *Ptx3*$^{+/+}$: 211 ± 13.9 pg/mL) were lesser in *Ptx3*$^{-/-}$ mice compared with those in *Ptx3*$^{+/+}$ mice on OVA challenge. However, the magnitude of IL-4 but not IL-5 induction as compared with their respective saline controls (data not shown) was greater in *Ptx3*$^{-/-}$ mice on OVA challenge in comparison with that seen in their *Ptx3*$^{+/+}$ littermates (see Fig E1, *A*, which shows a fold change in the concentration of IL-4 on OVA exposure in *Ptx3*$^{+/+}$ and *Ptx3*$^{-/-}$ mice).

OVA plus alum sensitization and challenge regimen preferentially generate a T_H2-skewed response over T_H1 or T_H17 responses.[17,18] As expected, *Ptx3*$^{+/+}$ OVA-challenged mice did not show considerable change in the concentration of IFN-γ (Fig 5, *B*) and IL-17A (Fig 5, *C*) in lung homogenates compared with their saline controls (IFN-γ OVA: 212.7 ± 7.8 pg/mL vs saline: 199.1 ± 10.1 pg/mL; IL-17A OVA: 190.2 ± 15.5 pg/mL vs saline: 172.4 ± 12.6 pg/mL). Lung homogenates from *Ptx3*$^{-/-}$ mice, on the other hand, showed a significant increase in concentrations of both cytokines on OVA exposure compared with those seen in their saline-exposed counterparts (IFN-γ OVA: 377.0 ± 38.6 pg/mL vs saline: not detected; IL-17A OVA: 176.8 ± 1.8 pg/mL vs saline: 35.6 ± 1.6 pg/mL; Fig 5, *B* and *C*, and see Fig E1, *B* and *C*). Concomitantly, an increase in IL-12 and IL-6 induction was also observed in *Ptx3*$^{-/-}$ mice on OVA exposure (see Fig E1, *E* and *F*, respectively).

Recall response in MLNs also demonstrated induction of IL-4, IFN-γ, and IL-17A responses in both strains. However, *Ptx3*$^{-/-}$ mice exhibited an IL-17A–prevalent response compared with their *Ptx3*$^{+/+}$ littermates (*Ptx3*$^{-/-}$: 2367 ± 184.2 pg/mL vs *Ptx3*$^{+/+}$: 966.7 ± 68.9 pg/mL; Fig 5, *F*). However, the absolute IFN-γ (Fig 5, *E*) response was similar in both genotypes on OVA challenge (*Ptx3*$^{-/-}$: 1902 ± 44.8 pg/mL vs *Ptx3*$^{+/+}$: 2052 ± 105.4 pg/mL). IL-4 (Fig 5, *D*) production was lower in P*tx3*$^{-/-}$ mice compared with their P*tx3*$^{+/+}$ littermates (*Ptx3*$^{-/-}$: 50 ± 11.5 pg/mL vs *Ptx3*$^{+/+}$: 78±21.3 pg/mL). Altogether, this suggests generation of a mixed proinflammatory response with an apparent dominance of T_H17 phenotype in *Ptx3*$^{-/-}$ mice in contrast to their wild-type counterparts on allergen exposure.

CD4 T cells from *Ptx3*$^{-/-}$ mice display enhanced activation and a T_H17-dominant phenotype

Given that CD4 T cells play a critical role in the production of proinflammatory cytokines in the lungs on allergen exposure,[19-21] we first explored activation status of CD4 T cells in *Ptx3*$^{+/+}$ and *Ptx3*$^{-/-}$ mice on OVA exposure. Lung CD4 T cells from *Ptx3*$^{-/-}$ mice showed an enhanced activated phenotype, as determined based on CD69 (Fig 5, *G* and *H*) and CD25 (Fig 5, *I* and *J*) expression,[22,23] compared with their wild-type counterparts. Also, OVA exposure induced enhanced generation of effector CD4 T cells in *Ptx3*$^{-/-}$ mice, as determined by $CD62L^{-}CD44^{int/high}$ staining (Fig 5, *K* and *L*). Flow cytometric analysis of cytokine-producing CD4 T cells showed that deletion of PTX3 allowed a significant expansion of IL-17A–producing CD4 T cells in OVA-induced inflammatory conditions (*Ptx3*$^{+/+}$: 0.096% ± 0.012% vs *Ptx3*$^{-/-}$: 0.27% ± 0.024% of total lung cells; Fig 5, *M* and *N*). Similar preponderance of the T_H17 phenotype was observed in the MLNs of *Ptx3*$^{-/-}$ mice (see Fig E2, *A* and *B*, in this article's Online Repository at www.jacionline.org). However, no significant difference was detected in the expansion of IL-4– and IFN-γ–producing lung CD4 T cells in both genotypes (see Fig E3, *A-D*, in this article's Online Repository at www.jacionline.org).

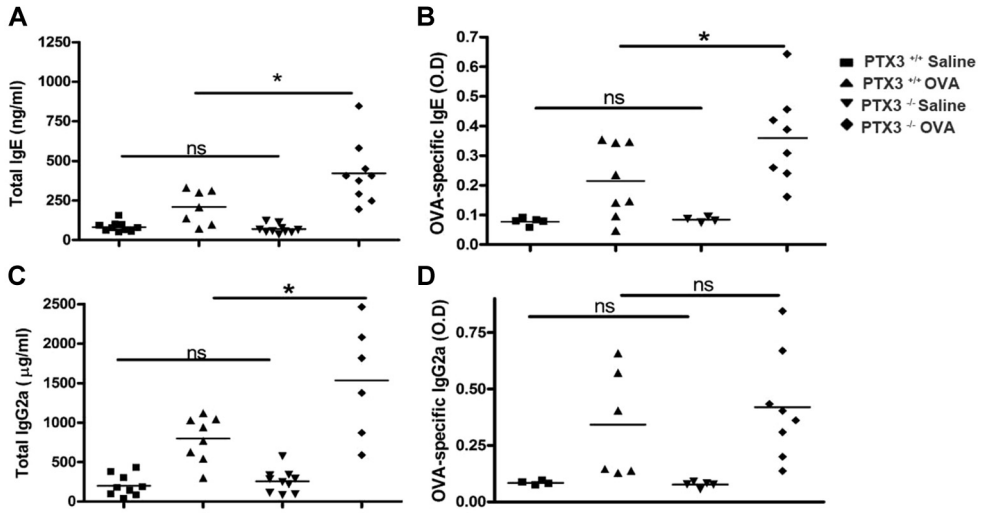

FIG 3. Total and OVA-specific IgE (**A** and **B**) and IgG_{2a} (**C** and **D**) levels were assessed in sera of saline- and OVA-exposed $Ptx3^{+/+}$ and $Ptx3^{-/-}$ mice by means of ELISA (n = 7-10 per group). *$P < .01$. *ns*, Not significant.

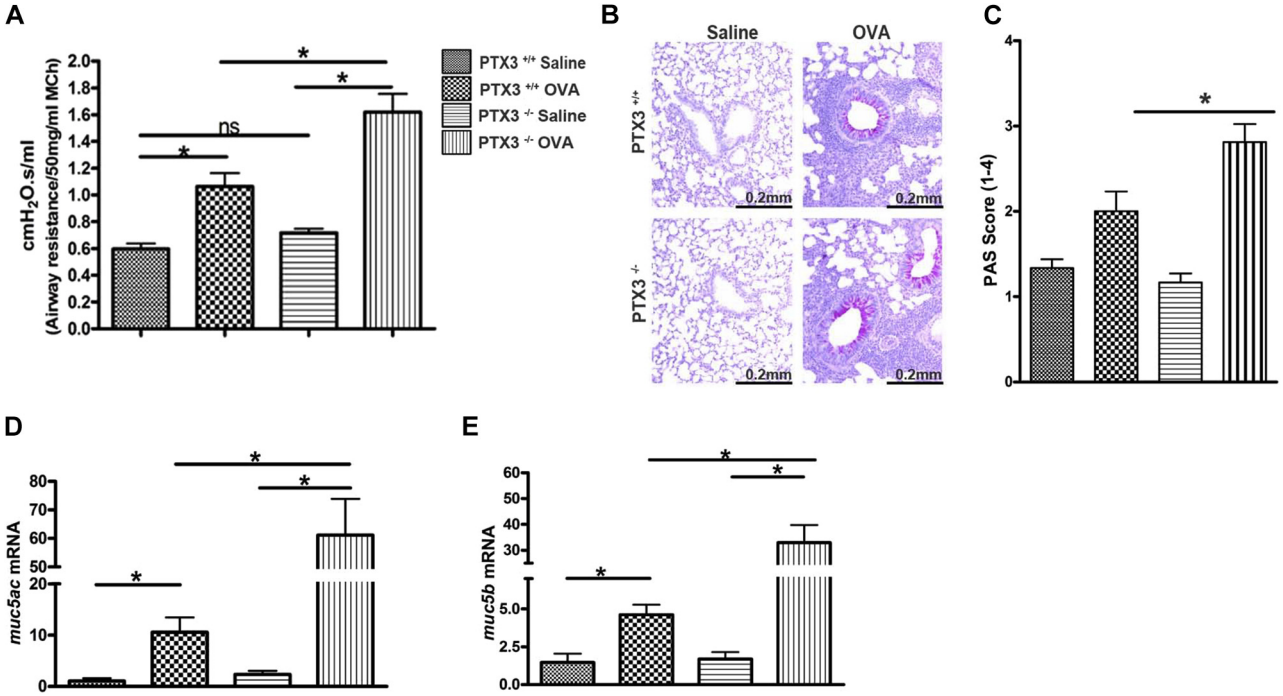

FIG 4. Deletion of PTX3 aggravates OVA-induced airway hyperreactivity and mucus gene expression. **A,** Airway resistance in OVA-sensitized/challenged $Ptx3^{+/+}$ and $Ptx3^{-/-}$ mice, as determined by using the flexiVENT small-animal ventilator. *ns*, Not significant. **B** and **C,** Mucus production in the lungs was determined by using PAS staining (×200 magnification). **D** and **E,** mRNA expression of the mucus genes *muc5ac* (Fig 4, *D*) and *muc5b* (Fig 4, *E*) was assessed by using real-time PCR (n = 12 per group). *$P < .01$.

IL-17A–producing CD4 T cells are uniquely characterized by a transcriptional program regulated by activation of signal transducer and activator of transcription 3 (STAT3)–dependent pathways.[24] We then investigated the status of STAT3 phosphorylation in the lungs of $Ptx3^{+/+}$ and $Ptx3^{-/-}$ mice in response to OVA. In contrast to saline-treated groups, phosphorylation of STAT3 was increased in the lungs of OVA-exposed $Ptx3^{-/-}$ mice compared with $Ptx3^{+/+}$ mice (see Fig E3, *E*).

Next, we investigated whether PTX3 deficiency favors the differentiation of CD4 T cells toward the T_H17 phenotype. Enriched naive spleen CD4 T cells from $Ptx3^{-/-}$ mice

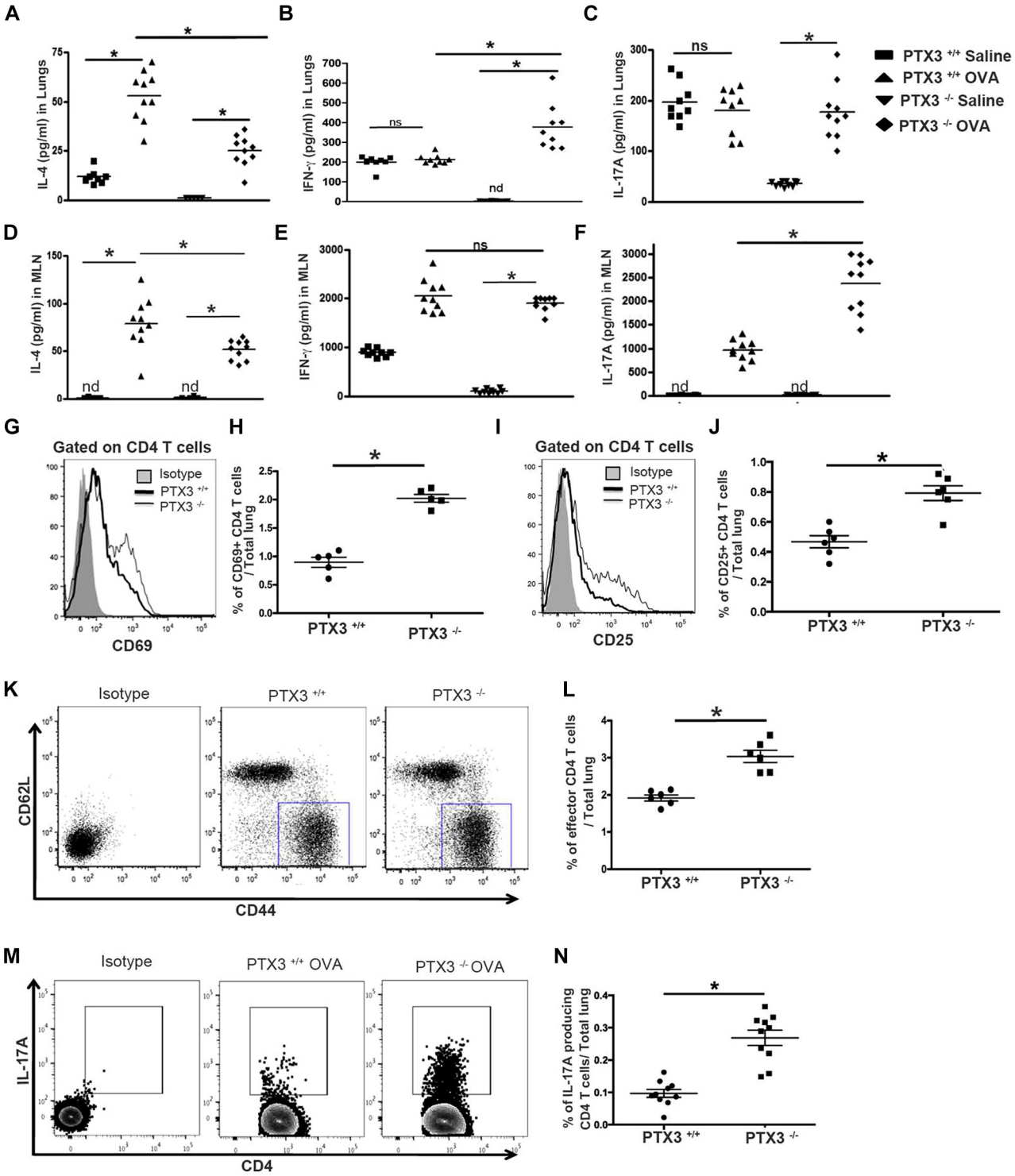

FIG 5. Absence of PTX3 induces enhanced IL-17A–dominant responses. **A-F,** Levels of proinflammatory cytokines in the lungs (Fig 5, *A-C*) and MLNs (Fig 5, *D-F*) were determined by means of ELISA (n = 8-10 mice per group). **G-J,** CD69 (Fig 5, *G* and *H*) and CD25 (Fig 5, *I* and *J*) expression on lung CD4 T cells (n = 5-6 mice per group). **K-N,** Characterization of effector lung CD4 T cells (Fig 5, *K* and *L*) and expression profile of IL-17A (Fig 5, *M* and *N*) by lung CD4 T cells in OVA-exposed *Ptx3*$^{+/+}$ and *Ptx3*$^{-/-}$ mice (n = 10 mice per group). *$P < .01$. *nd*, Not determined; *ns*, not significant.

(see Fig E3, *F*) exhibited enhanced T_H17 polarization when cultured in T_H17 polarization conditions compared with those from their *Ptx3*$^{+/+}$ counterparts (see Fig E3, *G* and *H*). Given that IL-6, a critical component of the T_H17 polarization cocktail, induces IL-17 production through a STAT3-dependent mechanism, we next assessed STAT3 phosphorylation in naive

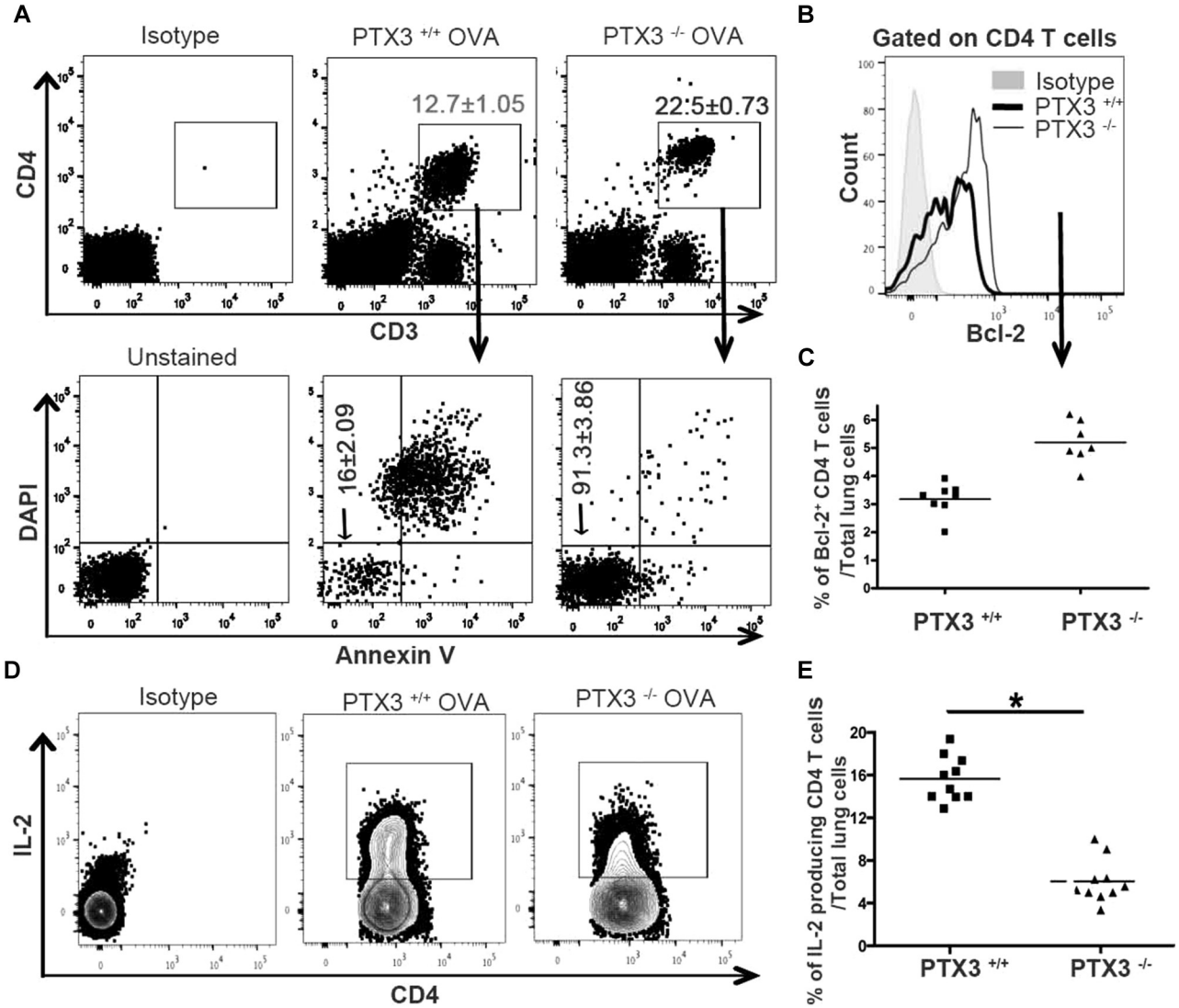

FIG 6. *Ptx3*$^{-/-}$ CD4 T cells show enhanced survival. **A,** Survival of lung CD4 T cells (CD3e^{+}CD4^{+}) was assessed by using Annexin V and 4′-6-diamisino-2-phenylindole dihydrochloride *(DAPI)* staining. Percentages of gated cells are presented as means ± SEMs (n = 8-10 per group). **B-E,** Expression of Bcl-2 (Fig 6, *B* and *C*) and IL-2 production (Fig 6, *D* and *E*) in OVA-exposed lung CD4 T cells were determined by means of flow cytometry. Quantification and statistical analysis of fluorescence-activated cell sorting data is shown as graphs (n = 5-10 per group). *$P < .01$.

CD4 T cells from *Ptx3*$^{-/-}$ and *Ptx3*$^{+/+}$ mice on IL-6 stimulation.[25,26] Parallel to our previous observation, we observed increased phosphorylation of STAT3 in naive CD4 T cells from *Ptx3*$^{-/-}$ mice on IL-6 stimulation compared with CD4 T cells from *Ptx3*$^{+/+}$ mice (see Fig E3, *I* and *J*). Together, these results suggest that deletion of PTX3 favors development of the T_H17 phenotype, possibly contributing to an IL-17A–dominant inflammatory response in the lungs and MLNs of *Ptx3*$^{-/-}$ mice on OVA exposure.

PTX3-deleted CD4 T cells exhibit enhanced survival

IL-17A through STAT3 promotes survival of various cells, including T cells, by upregulating prosurvival molecules, such as B-cell lymphoma 2 (Bcl-2).[27-29] Therefore we questioned whether the IL-17A–dominant phenotype, as observed in *Ptx3*$^{-/-}$ mice, results in altered survival of CD4 T cells. Lung cells were isolated from OVA-exposed *Ptx3*$^{+/+}$ and *Ptx3*$^{-/-}$ mice, cultured for 3 days in complete medium, and assessed for CD4 T-cell survival. OVA-exposed *Ptx3*$^{-/-}$ CD4 T cells displayed enhanced survival (Fig 6, *A*), as assessed by Annexin V and 4′-6-diamisino-2-phenylindole dihydrochloride staining. Naive CD4 T cells from *Ptx3*$^{-/-}$ mice also showed increased survival (see Fig E4 in this article's Online Repository at www.jacionline.org); however, such a survival benefit was more pronounced in OVA-challenged conditions. Together, it suggests that PTX3 deficiency is likely to confer an added survival advantage to CD4 T cells in OVA-exposed mice.

CD4 T cells from OVA-exposed *Ptx3*$^{-/-}$ mice exhibit enhanced expression of Bcl-2 and reduced production of IL-2

Bcl-2 is a prototypic member of a large Bcl-2 family that regulates T-cell apoptosis and helps maintain immune system homeostasis.[30,31] Therefore we examined whether the absence of PTX3 affects Bcl-2 expression in lung CD4 T cells. Although basal expression of Bcl-2 is comparable between CD4 T cells from *Ptx3*$^{-/-}$ and *Ptx3*$^{+/+}$ mice (see Fig E5, *A* and *B*, in this article's Online Repository at www.jacionline.org), OVA exposure induced greater expression of the prosurvival protein Bcl-2 in pulmonary CD4 T cells (Fig 6, *B* and *C*) from *Ptx3*$^{-/-}$ mice compared with those from *Ptx3*$^{+/+}$ mice, which is in parallel with enhanced survival (Fig 6, *A*). A previous study showed an association between IL-17A and enhanced survival of T cells by downregulating IL-2 production.[32] Subsequently, we examined IL-2 production by pulmonary CD4 T cells from OVA-exposed *Ptx3*$^{+/+}$ and *Ptx3*$^{-/-}$ mice. Consistent with the enhanced T_H17 phenotype and increased survival, OVA-exposed *Ptx3*$^{-/-}$ lungs (Fig 6, *D* and *E*) and MLNs (see Fig E2, *C* and *D*) CD4 T cells exhibited reduced IL-2 production. Similarly, CD4 T cells from *Ptx3*$^{-/-}$ mice exhibited reduced IL-2 production in the presence of T_H17 polarizations conditions compared with CD4 T cells from *Ptx3*$^{+/+}$ mice (see Fig E5, *C*). Collectively, our data showed enhanced Bcl-2 expression and reduced IL-2 production by lung CD4 T cells in *Ptx3*$^{-/-}$ mice, supporting their enhanced survival on OVA exposure.

DCs from *Ptx3*$^{-/-}$ mice produce increased levels of the T_H17-polarizing cytokines IL-6 and IL-23

In allergic inflammation DCs play a critical role in orchestrating pulmonary inflammation. In response to allergens, DCs produce CD4 T cell–polarizing cytokines and regulate polarization of naive CD4 T cells to differentiated CD4 T cells. IL-6, a proinflammatory cytokine produced by antigen-presenting cells, including DCs, induces differentiation of T_H17 CD4 T cells.[33] IL-23 acts subsequently and contributes to maintaining the T_H17 phenotype. Therefore our next aim was to understand whether DCs from *Ptx3*$^{-/-}$ mice regulate the generation of T_H17-dominant inflammation through altered IL-6 and IL-23 production. We compared production of IL-6 by DCs from *Ptx3*$^{-/-}$ and *Ptx3*$^{+/+}$ mice. P*tx3*$^{-/-}$ mice showed an increase in IL-6–producing (Fig 7, *B* and *C*) and IL-23–producing (Fig 7, *D* and *E*) lung CD11c^{+}CD11b^{+} DCs compared with that seen in DCs from *Ptx3*$^{+/+}$ mice. Similarly, there was increase in IL-6 (see Fig E6, *A*, *B*, *E*, and *F*, in this article's Online Repository at www.jacionline.org) and IL-23 (see Fig E6, *C*, *D*, *G*, and *H*) production in the draining lymph nodes of *Ptx3*$^{-/-}$ mice compared with that seen in *Ptx3*$^{+/+}$ mice on OVA exposure.

Because DCs from both *Ptx3*$^{-/-}$ and *Ptx3*$^{+/+}$ mice showed differential production of IL-6, we next asked whether these DCs would show differential ability to induce the T_H17 phenotype. We purified lung DCs from OVA-exposed *Ptx3*$^{+/+}$ and *Ptx3*$^{-/-}$ mice and cocultured them with carboxyfluorescein succinimidyl ester (CFSE)–labeled naive CD4 T cells from *Ptx3*$^{+/+}$ mice. The purity of naive CD4 T cells is shown in Fig E3, *F*. After 4 days of culture, naive CD4 T cells cocultured with DCs from *Ptx3*$^{-/-}$ mice showed a significant increase in the number of IL-17A–producing CD4 T cells (Fig 7, *F* and *G*) and production of IL-17A (Fig 7, *H*) compared with naive CD4 T cells cocultured with DCs from *Ptx3*$^{+/+}$ mice.

Coculture of DCs from OVA-exposed *Ptx3*$^{+/+}$ and *Ptx3*$^{-/-}$ mice with naive CD4 T cells from OTII mice also showed a similar response (Fig 7, *I* and *J*). Collectively, this suggests that T_H17-dominant allergic inflammation in *Ptx3*$^{-/-}$ mice was also attributed to augmented production of the T_H17-polarizing cytokines IL-6 and IL-23 by PTX3-depleted DCs.

DISCUSSION

The role of PTX3 in regulation of the innate immune system has been extensively investigated in the last decade. A key conclusion that has emerged from these findings is that PTX3 provides protection against specific infections, including SARS, *P aeruginosa*, CMV, pneumonia, and aspergillosis.[9] The role of PTX3 has not been previously studied in the mucosal adaptive immune response, particularly in asthmatic patients. In this report we revealed an association between PTX3 and allergic inflammation, as observed in asthmatic patients. Consistent with our BALF data from patients with severe allergic asthma, the lungs of allergen-exposed mice displayed a highly significant increase in the level of PTX3 compared with those of saline-treated control mice. These findings are in agreement with our previously reported data in bronchial biopsy specimens obtained from patients with severe asthma.[10] For the first time, we demonstrate that features of allergic asthma, such as AHR, airway remodeling, and inflammation, were heightened in the absence of PTX3 in a murine model of OVA-induced experimental asthma. Moreover, absence of PTX3 promotes a T_H17-dominant CD4 T-cell response in the lungs combined with enhanced survival of CD4 T cells, suggesting a critical function of PTX3 in preferential maintenance of the specific CD4 T-cell population, at least in OVA-induced inflammation. Enhanced production of IL-6 and IL-23 by DCs from mice deficient in PTX3, a T_H17-inducing proinflammatory cytokine, provides a mechanistic explanation accounting for an IL-17A–dominant allergic inflammation in these mice. Collectively, our data suggest a hitherto unrecognized function of PTX3 in regulation of events involved in the pathogenesis of asthma-associated allergic inflammation.

Compared with wild-type littermates, OVA-exposed *Ptx3*$^{-/-}$ mice showed enhanced inflammation, which was characterized by increased accumulation of neutrophils and eosinophils within the airways and lung tissue. This phenotype was accompanied by an IL-17A–dominant cytokine production. IL-17A, a prototype of the T_H17 phenotype, has been implicated in allergen-induced neutrophilia and eosinophilia, at least through production of chemokines, including keratinocyte chemoattractant,[34,35] which is a chemoattractant for neutrophils and eosinophils.[36,37] Along the same line, enhanced keratinocyte chemoattractant production (data not shown) was detected in the lungs of OVA-exposed *Ptx3*$^{-/-}$ mice, which might account for exaggerated neutrophilia and eosinophilia in *Ptx3*$^{-/-}$ mice. Previously, IL-17A was shown to enhance AHR through an airway smooth muscle–dependent mechanism.[38,39] Also, the IL-17 family is involved in upregulation of mucus genes, specifically *muc4ac* and *muc5b*.[40] These reports are in accord with an enhanced IL-17A–dominant response, increased AHR, and mucus production in OVA-exposed *Ptx3*$^{-/-}$ mice in comparison with *Ptx3*$^{+/+}$ mice.

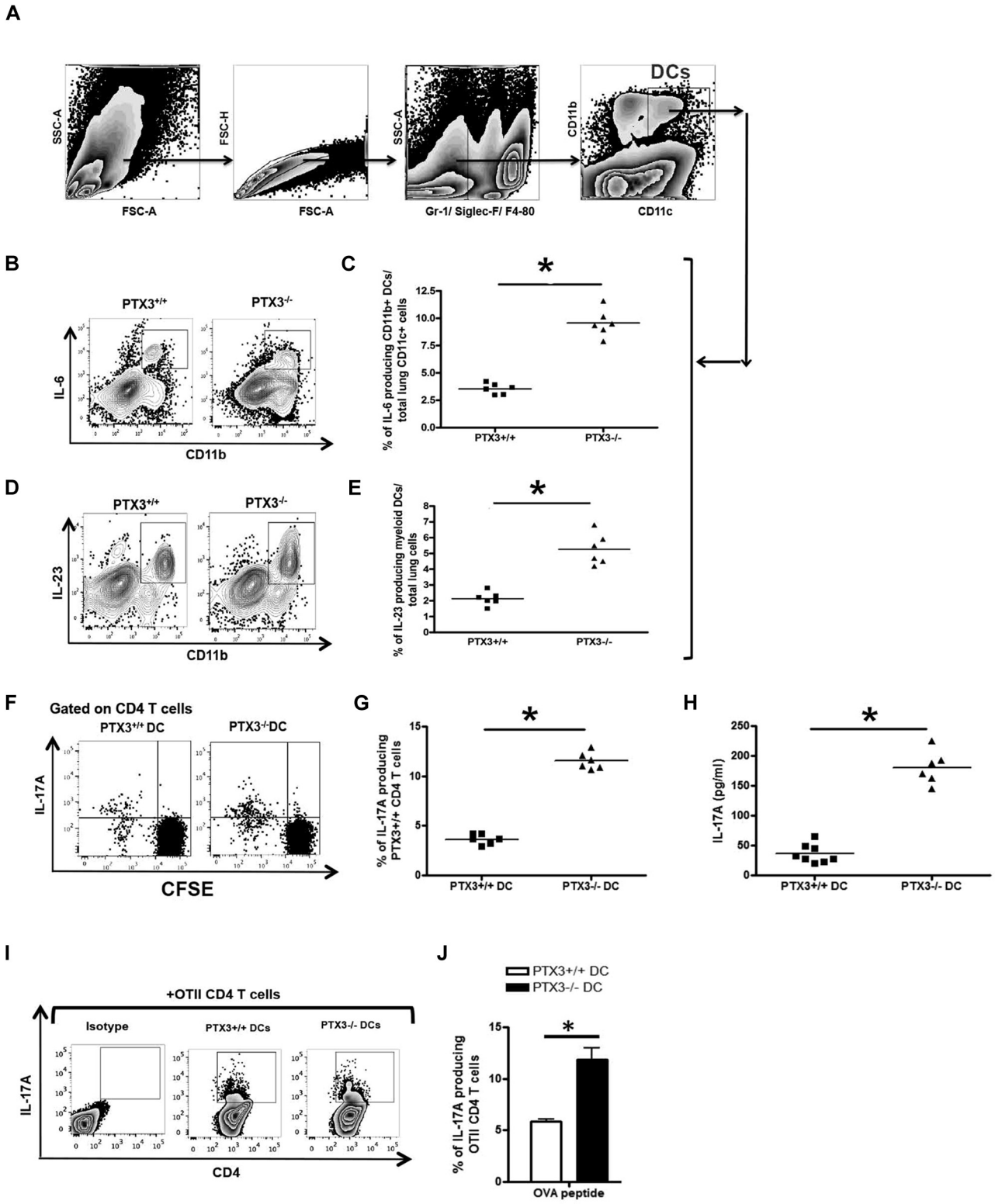

FIG 7. OVA exposure results in an increase in IL-6– and IL-23–producing DCs in *Ptx3*$^{-/-}$ mice. **A-E,** Lung CD11c^{+}CD11b^{+} DCs from OVA-exposed *Ptx3*$^{-/-}$ and *Ptx3*$^{+/+}$ mice (Fig 7, *A*) were assessed for the production of IL-6 (Fig 7, *B* and *C*) and IL-23 (Fig 7, *D* and *E*) by means of flow cytometry. *FSC*, Forward scatter; *SSC*, side scatter. **F** and **G,** Purified CFSE-labeled spleen naive CD4 T cells from *PTX3*$^{+/+}$ mice were cocultured with lung DCs from OVA-exposed *Ptx3*$^{-/-}$ and *Ptx3*$^{+/+}$ mice for 4 days, and numbers of IL-17A–producing CD4 T cells were quantified by using flow cytometry. **H,** IL-17A levels in these cocultures were detected by means of ELISA (n = 6-8 per group). **P* < .01. **I** and **J,** lung DCs from OVA-exposed *Ptx3*$^{-/-}$ and *Ptx3*$^{+/+}$ mice were cocultured with OTII mouse naive CD4 T cells, and the number of IL-17A–producing CD4 T cells was determined after 4 days (n = 3).

Lung CD4 T cells from OVA-exposed *Ptx3*$^{-/-}$ mice displayed enhanced activation compared with *Ptx3*$^{+/+}$ mice, as detected based on CD69 and CD25 surface staining. This result is in line with a recent study showing that PTX3 treatment suppressed CD25 and CD69 in OVA-specific CD4 T cells.[41] IL-17A production by CD4 T cells is mediated by a combination of IL-6/IL-23–dependent mechanisms[42,43] through at least STAT3 activation.[44] Heightened IL-17A production with an increased level of phosphorylated STAT3 in the lungs of OVA-exposed *Ptx3*$^{-/-}$ mice is in accordance with previously published data.

IL-2 is a key negative regulator of the T_H17 phenotype[45] that is suppressed by STAT3 activation in T cells.[32] Indeed, compared with *Ptx3*$^{+/+}$ mice, reduced production of IL-2 in CD4 T cells from OVA-exposed *Ptx3*$^{-/-}$ mice was observed, which might provide a reasonable mechanism accounting for the enhanced IL-17A production and STAT3 activation in our model. In concert with our observation, Moalli et al[46] and Paroni et al[47] reported reduced IL-17A levels on treatment with exogenous PTX3 in murine models of chronic *P aeruginosa* lung infection and cystic fibrosis, respectively. Our findings combined with the above studies suggest an inverse correlation between PTX3 and the IL-17A–dependent pathway. Also, D'Angelo et al[48] and Zhu et al[49] showed that PTX3 suppressed IL-17A–mediated inflammation in *Aspergillus* species–induced chronic granulomatous disease and an ischemia reperfusion injury model, respectively. Although both later studies mainly suggested that PTX3 suppressed IL-17A production by restricting γδ T-cell expansion, our study highlights a novel function of PTX3 in the regulation of IL-17A production by CD4 T cells. Altogether, the data point to a unique function of PTX3 in counterregulating IL-17A/T_H17–dominant immune response.

Development of the immune response in asthmatic airways is primarily driven by increased cell infiltration, prolonged survival of proinflammatory cells, or both.[50] Cell death of proinflammatory cells is a regulatory mechanism that limits inflammation-induced tissue injury and promotes resolution.[50] Enhanced survival of T cells has been reported in the airways of asthmatic patients.[51-53] Furthermore, BALF T cells from allergen-exposed asthmatic patients were shown to be less susceptible to apoptosis-inducing agents through Bcl-2–enhanced expression.[54] In our study we found that CD4 T cells from OVA-exposed P*tx*3$^{-/-}$ mice are more resistant to postactivation-induced apoptosis and displayed increased Bcl-2 expression. This phenomenon is in accordance with enhanced IL-17A production, STAT3 phosphorylation, and reduced IL-2 production observed in *Ptx3*$^{-/-}$ mice, which are key factors implicated in T-cell survival.[32,55,56]

Previously, Lech et al[57] reported splenomegaly and lymph node hyperplasia in *Ptx3/lpr*$^{-/-}$ mice in systemic lupus erythematosus, which was also associated with exaggerated inflammation in the lungs. Whether this was due to an enhanced survival of lymphocytes in the absence of PTX3 will be interesting to study. The analysis conducted herein suggests greater longevity of CD4 T cells from *Ptx3*$^{-/-}$ mice that can drive enhanced allergen-induced airway inflammation in *Ptx3*$^{-/-}$ mice.

Despite the fact that CD4 T cells from *Ptx3*$^{-/-}$ mice show increased IL-17A production and the accompanying phenotype characterized by enhanced STAT3 phosphorylation, survival, and reduced IL-2 production in OVA-induced inflammatory condition, PTX3 deletion does not seem to substantially affect these pathways in naive conditions. It is likely that a unique phenotype of CD4 T cells from *Ptx3*$^{-/-}$ mice, as observed in inflammation, can result from alteration of other cell types. DCs constitute major antigen (allergen)–presenting cells to T cells in allergic inflammation. Besides presenting allergen epitopes and providing costimulatory signals, they regulate the phenotype and functions of CD4 T cells through cytokine production. DCs produce IL-6 and IL-23, through which these cells dictate differentiation of naive CD4 T cells to T_H17 CD4 T cells through activation of STAT3-dependent pathway.[25,58] Increased numbers of IL-6– and IL-23–producing DCs in the lungs of *Ptx3*$^{-/-}$ mice on OVA exposure explain the enhanced differentiation of T_H17 cells in OVA-exposed *Ptx3*$^{-/-}$ mice compared with that seen in wild-type control mice. Altogether, our data suggest contribution of DCs from *Ptx3*$^{-/-}$ mice through increased IL-6 production, resulting in IL-17A–prominent inflammation. However, we do not deny role of other IL-6– and IL-23–producing structural and inflammatory cells, including epithelial cells and macrophages, respectively. Whether they also regulate IL-17A–dominant inflammation in P*tx*3$^{-/-}$ mice will be interesting to study in succeeding studies.

Together, it seems that IL-17A–dominant inflammatory responses in *Ptx3*$^{-/-}$ mice compared with *Ptx3*$^{+/+}$ mice might have stemmed from 2 plausible mechanisms. CD4 T cells from *Ptx3*$^{-/-}$ mice are able to induce increased STAT3 phosphorylation and IL-17A production when exposed to IL-6 and the T_H17 polarization cocktail, respectively. This suggests an altered programing of CD4 T cells on PTX3 deletion that might lead to IL-17A–dominant CD4 T cells phenotype in these mice. *In vivo* increased IL-6 and IL-23 production by DCs from *Ptx3*$^{-/-}$ mice, which are known to promote IL-17A production, serves as an additional mechanism.

Very recently, Cinha et al[59] reported the existence of the G-A/G-A (h2/h2) single nucleotide polymorphism (SNP) in hematopoietic stem cell transplant donors, which renders recipients more susceptible to invasive pulmonary aspergillosis. The h2/h2 SNP resulted in PTX3 deficiency that affected antifungal function of neutrophils in transplant recipients. Whether the h2/h2 SNP has an effect on allergen-induced inflammation is worth questioning.

In summary, our study assigns a critical function of PTX3 in the cause of allergic inflammation. Without dismissing the role of PTX3 in regulating innate inflammatory mechanisms, our study proposes that the absence of PTX3 results in dysregulated programming of CD4 T cells, leading to an exaggerated allergen-induced inflammation. The IL-17A–dominant immune response has previously been associated with steroid-resistant severe asthma in human subjects.[60] Therefore our study might provide some novel insight into understanding the mechanisms involved in regulation of the IL-17A–dominant immune response in patients with severe asthma. Based on our current data, it is difficult to infer whether PTX3 treatment would provide protection against unwarranted allergen-induced activation of immune system. However, our data clearly show that deletion of PTX3 plays a critical role in regulating functional capacity of immune system, thereby affecting immunologic metrics in response to an allergen in a murine model of experimental asthma.

We thank Christine Zhang, Vidyanand Anaparthi, Sujata Basu, Abeer Saati, Mohammad Ashfaque, Hesam Movassagh, and Nazanin Tatari for technical help.

Key messages

- **PTX3 levels increase in the airways of patients with severe asthma and OVA-exposed mice.**
- **Deletion of PTX3 results in enhanced inflammation, AHR, and mucus production on OVA sensitization and challenge.**
- **OVA exposure induces a T_H17-dominant immune response in *Ptx3*$^{-/-}$ mice compared with *Ptx3*$^{+/+}$ mice.**
- **On OVA exposure, CD4 T cells from *Ptx3*$^{-/-}$ mice exhibit an enhanced survival in contrast to *Ptx3*$^{+/+}$ mice.**
- **DCs from *Ptx3*$^{-/-}$ mice produce greater levels of the T_H17-polarizing cytokines IL-6 and IL-23, plausibly promoting T_H17-dominant inflammation in the PTX3-depleted condition.**

REFERENCES

1. Braman SS. The global burden of asthma. Chest 2006;130(suppl):4S-12S.
2. Palmer LJ, Burton PR, Faux JA, James AL, Musk AW, Cookson WO. Independent inheritance of serum immunoglobulin E concentrations and airway responsiveness. Am J Respir Crit Care Med 2000;161:1836-43.
3. Duffy DL, Martin NG, Battistutta D, Hopper JL, Mathews JD. Genetics of asthma and hay fever in Australian twins. Am Rev Respir Dis 1990;142:1351-8.
4. Worldwide variation in prevalence of symptoms of asthma, allergic rhinoconjunctivitis, and atopic eczema: ISAAC. The International Study of Asthma and Allergies in Childhood (ISAAC) Steering Committee. Lancet 1998;351:1225-32.
5. Sha Q, Truong-Tran AQ, Plitt JR, Beck LA, Schleimer RP. Activation of airway epithelial cells by toll-like receptor agonists. Am J Respir Cell Mol Biol 2004;31:358-64.
6. Akira S. Pathogen recognition by innate immunity and its signaling. Proc Jpn Acad Ser B Phys Biol Sci 2009;85:143-56.
7. Lam D, Ng N, Lee S, Batzer G, Horner AA. Airway house dust extract exposures modify allergen-induced airway hypersensitivity responses by TLR4-dependent and independent pathways. J Immunol 2008;181:2925-32.
8. Holgate ST. Innate and adaptive immune responses in asthma. Nat Med 2012;18:673-83.
9. Balhara J, Koussih L, Zhang J, Gounni AS. Pentraxin 3: an immuno-regulator in the lungs. Front Immunol 2013;4:127.
10. Zhang J, Shan L, Koussih L, Redhu NS, Halayko AJ, Chakir J, et al. Pentraxin 3 (PTX3) expression in allergic asthmatic airways: role in airway smooth muscle migration and chemokine production. PLoS One 2012;7:e34965.
11. Kadkhoda K, Wang S, Fan Y, Qiu H, Basu S, Halayko AJ, et al. ICOS ligand expression is essential for allergic airway hyperresponsiveness. Int Immunol 2011;23:239-49.
12. Luo HR, Loison F. Constitutive neutrophil apoptosis: mechanisms and regulation. Am J Hematol 2008;83:288-95.
13. Bacharier LB, Geha RS. Molecular mechanisms of IgE regulation. J Allergy Clin Immunol 2000;105(suppl):S547-58.
14. Coffman RL, Lebman DA, Rothman P. Mechanism and regulation of immunoglobulin isotype switching. Adv Immunol 1993;54:229-70.
15. Truyen E, Coteur L, Dilissen E, Overbergh L, Dupont LJ, Ceuppens JL, et al. Evaluation of airway inflammation by quantitative Th1/Th2 cytokine mRNA measurement in sputum of asthma patients. Thorax 2006;61:202-8.
16. Finkelman FD, Hogan SP, Hershey GK, Rothenberg ME, Wills-Karp M. Importance of cytokines in murine allergic airway disease and human asthma. J Immunol 2010;184:1663-74.
17. Brewer JM, Conacher M, Hunter CA, Mohrs M, Brombacher F, Alexander J. Aluminium hydroxide adjuvant initiates strong antigen-specific Th2 responses in the absence of IL-4- or IL-13-mediated signaling. J Immunol 1999;163:6448-54.
18. Kool M, Soullie T, van Nimwegen M, Willart MA, Muskens F, Jung S, et al. Alum adjuvant boosts adaptive immunity by inducing uric acid and activating inflammatory dendritic cells. J Exp Med 2008;205:869-82.
19. Brown V, Warke TJ, Shields MD, Ennis M. T cell cytokine profiles in childhood asthma. Thorax 2003;58:311-6.
20. Zhu J, Paul WE. CD4 T cells: fates, functions, and faults. Blood 2008;112:1557-69.
21. Kay AB. T cells as orchestrators of the asthmatic response. Ciba Found Symp 1997;206:56-67, discussion 67-70, 106-10.
22. Ziegler SF, Ramsdell F, Alderson MR. The activation antigen CD69. Stem Cells 1994;12:456-65.
23. Caruso A, Licenziati S, Corulli M, Canaris AD, De Francesco MA, Fiorentini S, et al. Flow cytometric analysis of activation markers on stimulated T cells and their correlation with cell proliferation. Cytometry 1997;27:71-6.
24. Yang XP, Ghoreschi K, Steward-Tharp SM, Rodriguez-Canales J, Zhu J, Grainger JR, et al. Opposing regulation of the locus encoding IL-17 through direct, reciprocal actions of STAT3 and STAT5. Nat Immunol 2011;12:247-54.
25. Yang XO, Panopoulos AD, Nurieva R, Chang SH, Wang D, Watowich SS, et al. STAT3 regulates cytokine-mediated generation of inflammatory helper T cells. J Biol Chem 2007;282:9358-63.
26. Mathur AN, Chang HC, Zisoulis DG, Stritesky GL, Yu Q, O'Malley JT, et al. Stat3 and Stat4 direct development of IL-17-secreting Th cells. J Immunol 2007;178:4901-7.
27. Hou W, Jin YH, Kang HS, Kim BS. Interleukin-6 (IL-6) and IL-17 synergistically promote viral persistence by inhibiting cellular apoptosis and cytotoxic T cell function. J Virol 2014;88:8479-89.
28. Lee SY, Kwok SK, Son HJ, Ryu JG, Kim EK, Oh HJ, et al. IL-17-mediated Bcl-2 expression regulates survival of fibroblast-like synoviocytes in rheumatoid arthritis through STAT3 activation. Arthritis Res Ther 2013;15:R31.
29. Sergejeva S, Ivanov S, Lotvall J, Linden A. Interleukin-17 as a recruitment and survival factor for airway macrophages in allergic airway inflammation. Am J Respir Cell Mol Biol 2005;33:248-53.
30. Danial NN. BCL-2 family proteins: critical checkpoints of apoptotic cell death. Clin Cancer Res 2007;13:7254-63.
31. Marsden VS, Strasser A. Control of apoptosis in the immune system: Bcl-2, BH3-only proteins and more. Annu Rev Immunol 2003;21:71-105.
32. Oh HM, Yu CR, Golestaneh N, Amadi-Obi A, Lee YS, Eseonu A, et al. STAT3 protein promotes T-cell survival and inhibits interleukin-2 production through up-regulation of Class O Forkhead transcription factors. J Biol Chem 2011;286:30888-97.
33. Lewkowich IP, Lajoie S, Clark JR, Herman NS, Sproles AA, Wills-Karp M. Allergen uptake, activation, and IL-23 production by pulmonary myeloid DCs drives airway hyperresponsiveness in asthma-susceptible mice. PLoS One 2008;3:e3879.
34. Gu Y, Hu X, Liu C, Qv X, Xu C. Interleukin (IL)-17 promotes macrophages to produce IL-8, IL-6 and tumour necrosis factor-alpha in aplastic anaemia. Br J Haematol 2008;142:109-14.
35. Yao Z, Painter SL, Fanslow WC, Ulrich D, Macduff BM, Spriggs MK, et al. Human IL-17: a novel cytokine derived from T cells. J Immunol 1995;155:5483-6.
36. Erger RA, Casale TB. Interleukin-8 is a potent mediator of eosinophil chemotaxis through endothelium and epithelium. Am J Physiol Lung Cell Mol Physiol 1995;268:L117-22.
37. Hammond ME, Lapointe GR, Feucht PH, Hilt S, Gallegos CA, Gordon CA, et al. IL-8 induces neutrophil chemotaxis predominantly via type I IL-8 receptors. J Immunol 1995;155:1428-33.
38. Kudo M, Melton AC, Chen C, Engler MB, Huang KE, Ren X, et al. IL-17A produced by alphabeta T cells drives airway hyper-responsiveness in mice and enhances mouse and human airway smooth muscle contraction. Nat Med 2012;18:547-54.
39. Mizutani N, Nabe T, Yoshino S. IL-17A promotes the exacerbation of IL-33-induced airway hyperresponsiveness by enhancing neutrophilic inflammation via CXCR2 signaling in mice. J Immunol 2014;192:1372-84.
40. Chen Y, Thai P, Zhao YH, Ho YS, DeSouza MM, Wu R. Stimulation of airway mucin gene expression by interleukin (IL)-17 through IL-6 paracrine/autocrine loop. J Biol Chem 2003;278:17036-43.
41. He H, Tan Y, Duffort S, Perez VL, Tseng SC. *In vivo* downregulation of innate and adaptive immune responses in corneal allograft rejection by HC-HA/PTX3 complex purified from amniotic membrane. Invest Ophthalmol Vis Sci 2014;55:1647-56.
42. Mus AM, Cornelissen F, Asmawidjaja PS, van Hamburg JP, Boon L, Hendriks RW, et al. Interleukin-23 promotes Th17 differentiation by inhibiting T-bet and FoxP3 and is required for elevation of interleukin-22, but not interleukin-21, in autoimmune experimental arthritis. Arthritis Rheum 2010;62:1043-50.
43. Zhou L, Ivanov II, Spolski R, Min R, Shenderov K, Egawa T, et al. IL-6 programs T(H)-17 cell differentiation by promoting sequential engagement of the IL-21 and IL-23 pathways. Nat Immunol 2007;8:967-74.

44. Pappu R, Ramirez-Carrozzi V, Ota N, Ouyang W, Hu Y. The IL-17 family cytokines in immunity and disease. J Clin Immunol 2010;30:185-95.
45. Boyman O, Sprent J. The role of interleukin-2 during homeostasis and activation of the immune system. Nat Rev Immunol 2012;12:180-90.
46. Moalli F, Paroni M, Veliz Rodriguez T, Riva F, Polentarutti N, Bottazzi B, et al. The therapeutic potential of the humoral pattern recognition molecule PTX3 in chronic lung infection caused by *Pseudomonas aeruginosa*. J Immunol 2011; 186:5425-34.
47. Paroni M, Moalli F, Nebuloni M, Pasqualini F, Bonfield T, Nonis A, et al. Response of CFTR-deficient mice to long-term chronic Pseudomonas aeruginosa infection and PTX3 therapy. J Infect Dis 2013;208:130-8.
48. D'Angelo C, De Luca A, Zelante T, Bonifazi P, Moretti S, Giovannini G, et al. Exogenous pentraxin 3 restores antifungal resistance and restrains inflammation in murine chronic granulomatous disease. J Immunol 2009;183:4609-18.
49. Zhu H, Cui D, Liu K, Wang L, Huang L, Li J. Long pentraxin PTX3 attenuates ischemia reperfusion injury in a cardiac transplantation model. Transpl Int 2014; 27:87-95.
50. Bidere N, Su HC, Lenardo MJ. Genetic disorders of programmed cell death in the immune system. Annu Rev Immunol 2006;24:321-52.
51. Vignola AM, Chanez P, Chiappara G, Siena L, Merendino A, Reina C, et al. Evaluation of apoptosis of eosinophils, macrophages, and T lymphocytes in mucosal biopsy specimens of patients with asthma and chronic bronchitis. J Allergy Clin Immunol 1999;103:563-73.
52. Cormican L, O'Sullivan S, Burke CM, Poulter LW. IFN-gamma but not IL-4 T cells of the asthmatic bronchial wall show increased incidence of apoptosis. Clin Exp Allergy 2001;31:731-9.
53. Hamzaoui A, Hamzaoui K, Salah H, Chabbou A. Lymphocytes apoptosis in patients with acute exacerbation of asthma. Mediators Inflamm 1999;8: 237-43.
54. Muller M, Grunewald J, Olgart Hoglund C, Dahlen B, Eklund A, Stridh H. Altered apoptosis in bronchoalveolar lavage lymphocytes after allergen exposure of atopic asthmatic subjects. Eur Respir J 2006;28:513-22.
55. Boggio E, Clemente N, Mondino A, Cappellano G, Orilieri E, Gigliotti CL, et al. IL-17 protects T cells from apoptosis and contributes to development of ALPS-like phenotypes. Blood 2014;123:1178-86.
56. Lenardo MJ. Interleukin-2 programs mouse alpha beta T lymphocytes for apoptosis. Nature 1991;353:858-61.
57. Lech M, Rommele C, Kulkarni OP, Susanti HE, Migliorini A, Garlanda C, et al. Lack of the long pentraxin PTX3 promotes autoimmune lung disease but not glomerulonephritis in murine systemic lupus erythematosus. PLoS One 2011;6: e20118.
58. Perona-Wright G, Jenkins SJ, O'Connor RA, Zienkiewicz D, McSorley HJ, Maizels RM, et al. A pivotal role for CD40-mediated IL-6 production by dendritic cells during IL-17 induction *in vivo*. J Immunol 2009;182: 2808-15.
59. Cunha C, Aversa F, Lacerda JF, Busca A, Kurzai O, Grube M, et al. Genetic PTX3 deficiency and aspergillosis in stem-cell transplantation. N Engl J Med 2014;370: 421-32.
60. Chambers ES, Nanzer AM, Pfeffer PE, Richards DF, Timms PM, Martineau AR, et al. Distinct endotypes of steroid-resistant asthma characterized by IL-17A(high) and IFN-gamma(high) immunophenotypes: potential benefits of calcitriol. J Allergy Clin Immunol 2015;136:628-37.e4.

METHODS

Lung mechanics

To determine whether OVA exposure has different effects on respiratory mechanics in *Ptx3*$^{+/+}$ and *Ptx3*$^{-/-}$ mice, we performed aerosol MCh challenges using a flexiVent small-animal ventilator (SCIREQ, Montreal, Quebec, Canada). Mice were anesthetized intraperitoneally (pentobarbital, 0.1 mL per 10 g of body weight). After establishing anesthesia, midcervical tracheotomy was performed by inserting a polyethylene catheter (1.1 × 25 mm), which was kept in place by ligating with surgical silk thread. The catheter was connected to the small-animal ventilator, and positive end-expiratory pressure was maintained at 3 cm H_2O. Mice were subjected to serial aerosol MCh challenge (30 μL, 3-50 mg · mL^{-1} MCh in saline), and baseline mechanics were determined by using saline-only challenge. Before each challenge with saline or MCh, lung loading history was normalized by means of inflation to total lung capacity. Respiratory mechanics were assessed by using a preset flexiVent Prime-8 low-frequency forced oscillation protocol to derive respiratory mechanical input impedance. Airway resistance was derived by fitting respiratory mechanical input impedance to the constant-phase model.

BALF collection from mice

Mouse tracheas were cannulated with a 20-gauge catheter and tied in place with a surgical thread. The lungs were washed 2 times with 1 mL of PBS, and we obtained approximately 700 μL of fluid from each wash. BALF was centrifuged at 1000 rpm for 10 minutes, and the supernatant was used for ELISA. The pellet was resuspended in 500 μL of PBS for counting and used for BAL smear preparation. To determine numbers of different immune cells, such as eosinophils, basophils, and neutrophils, the BAL smear was fixed and stained with a Hema-3 stain set (Fisher Scientific, Waltham, Mass). These inflammatory cells were counted based on cellular morphology and staining characteristics.

Lung homogenate collection

Left lung lobes were collected from OVA-exposed and control mice and homogenized in a glass homogenizer in 2 mL of PBS. The homogenate was centrifuged at 500 rpm, followed by supernatant collection and storage at −80°C for cytokine measurement by means of ELISA.

Serum collection

Blood was collected and coagulated at 4°C, followed by centrifugation for 20 minutes at 7500 rpm. Circulating total and anti-OVA IgE and IgG subclasses were measured in the sera by means of ELISA. Ninety-six-well plates were coated overnight at 4°C with 50 μL of 0.1 mol/L $NaHCO_3$ containing 100 μg of OVA/mL. Then plates were blocked for 2 hours at 37°C with 200 μL of 3% BSA in PBS. Plates were washed, and 50 μL of 4 series with 10-fold serum dilutions for anti-OVA and 1:20,000 for total IgE and IgG_{2a} in PBS containing 1% BSA was applied overnight at 4°C. The amount of bound antibody was analyzed by using horseradish peroxidase–conjugated antibodies against mouse heavy chain classes.

Ex vivo MLN cell culture

Ptx3$^{+/+}$ and *Ptx3*$^{-/-}$ mice were challenged with OVA in alum adjuvant, and then MLNs were collected. RBCs were lysed by incubating MLN cells in NH_4Cl solution. Cells were then cultured in complete RPMI at 5 × 10^6 cells/mL in a 48-well plate and treated with OVA (50 μg/mL) for 72 hours, and the supernatant was then collected and stored.

Survival assay

A single-cell suspension of lung cells was cultured for 3 days in complete medium. Apoptosis/survival of CD4 T cells was determined by staining with Annexin V and 4′-6-diamisino-2-phenylindole dihydrochloride with the Apoptosis Detection kit FITC from eBioscience, according to the manufacturer's instructions.

In vitro T_H17 polarization assay

Naive CD4 T cells were enriched from murine splenocytes by using naive CD4 T Cell Negative Selection Kit (Miltenyi Biotec, Bergisch Gladbach, Germany) and cultured for 5 days in the presence of IL-6 (100 ng/mL, eBioscience), TGF-β (10 ng/mL; R&D Systems, Minneapolis, Min), anti–IL-4 (10 μg/mL, eBioscience), anti–IFN-γ (10 μg/mL, eBioscience), anti-CD3e (2 μg/mL, eBioscience), and anti-CD28 (2 μg/mL, eBioscience) in round-bottom 96-well plates.[E1]

CD4 T cell–DC coculture

Purified naive CD4 T cells from *Ptx3*$^{+/+}$ mice were cocultured with purified DCs from the lungs of OVA-exposed *Ptx3*$^{+/+}$ and *Ptx3*$^{-/-}$ mice. DCs were sorted with a FACSAria as CD11c$^+$CD11b$^+$ Gr-1$^-$F4/80$^-$Siglec F$^-$, as shown in Fig 7, *A*. The purity of naive CD4 T cells is shown in Fig E3, *F*. Supernatants from cocultured cells were collected after 4 days, and IL-17A levels were detected by means of ELISA.

CFSE staining

Three to 10 million naive CD4 T cells were resuspended in 5 mL of serum free media or PBS, and 3 μmol/L CFSE in 5 mL of PBS or serum free media was added. The total 10-mL mixture was incubated in the dark at room temperature for 8 minutes. Thereafter, 5 mL of FBS was added and centrifuged at 1200 rpm for 5 minutes, and the pellet was then resuspended in complete cell-culture media. Cells were washed 1 more time. There were 200,000 cells/100 μL CFSE-labeled naive CD4 T cells in each well of a round-bottom 96-well plate.

mRNA analysis

Total cellular RNA from lungs was obtained with Trizol Reagent (Invitrogen, Carlsbad, Calif). mRNA expression of specific genes (*muc5ac* and *muc5b)* was evaluated by means of real-time PCR with specific primers on an ABI RT-PCR machine (Table E2).

REFERENCE

E1. Quintana FJ, Jin H, Burns EJ, Nadeau M, Yeste A, Kumar D, et al. Aiolos promotes TH17 differentiation by directly silencing Il2 expression. Nat Immunol 2012;13:770-7.

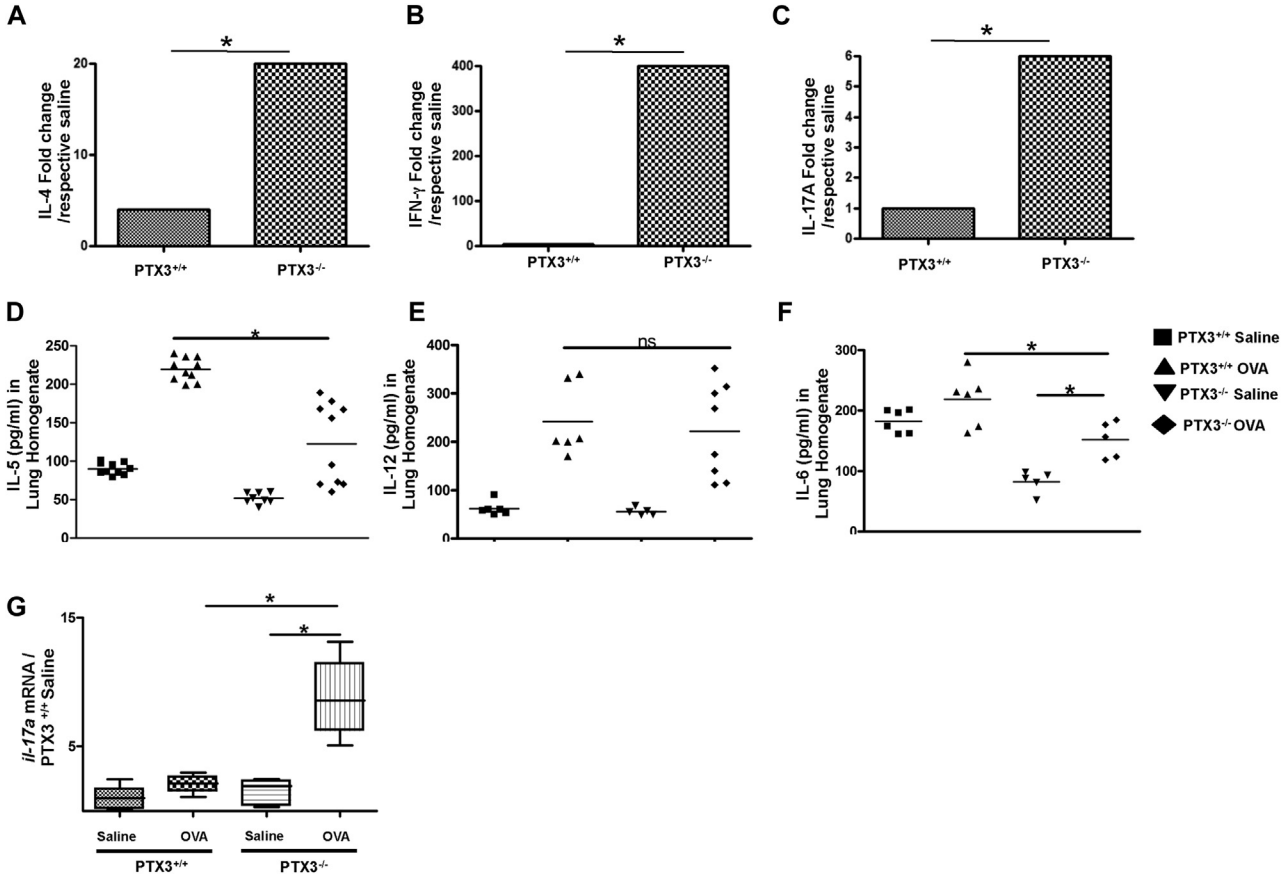

FIG E1. A-C, Fold increase in cytokine levels after exposure to OVA compared with respective saline control levels in *Ptx3*$^{+/+}$ and *Ptx3*$^{-/-}$ mice. **D-F,** Concentrations of IL-5 (Fig E1, *D*), IL-12 (Fig E1, *E*), and IL-6 (Fig E1, *F*) in the lungs of *Ptx3*$^{+/+}$ and *Ptx3*$^{-/-}$ mice, as determined by means of ELISA (n = 5-10 per group). *$P < .01$. **G,** mRNA level of IL-17A, as assessed by using real-time PCR, in the lungs of *Ptx3*$^{+/+}$ and *Ptx3*$^{-/-}$ mice in saline- and OVA-exposed conditions (n = 8-12 per group). *$P < .01$. *ns*, Not significant.

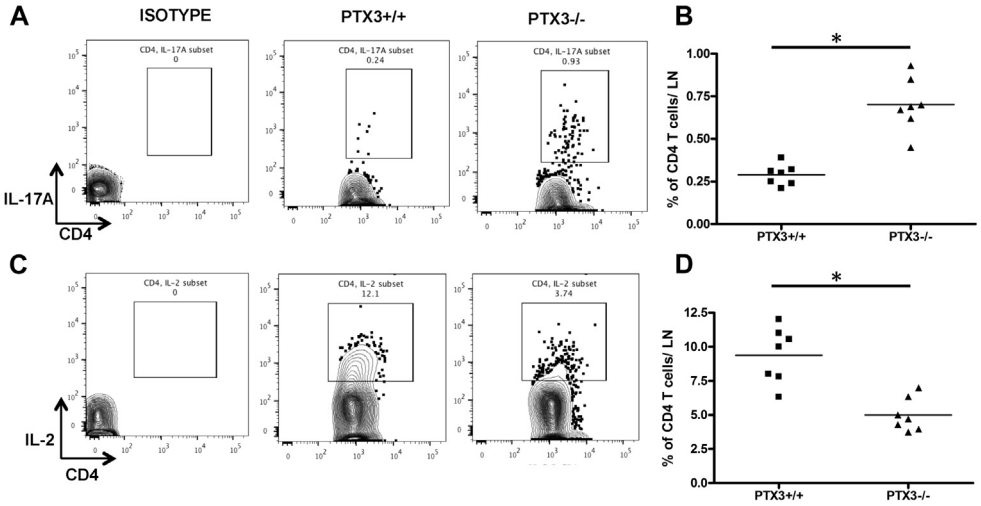

FIG E2. Flow cytometric analysis of expression profiles of IL-17A (**A** and **B**) and IL-2 (**C** and **D**) by MLN CD4 T cells from OVA-exposed *Ptx3*$^{+/+}$ and *Ptx3*$^{-/-}$ mice. Quantification and statistical analysis of fluorescence-activated cell sorting data is shown as graphs (n = 6-8/group). *$P < .01$.

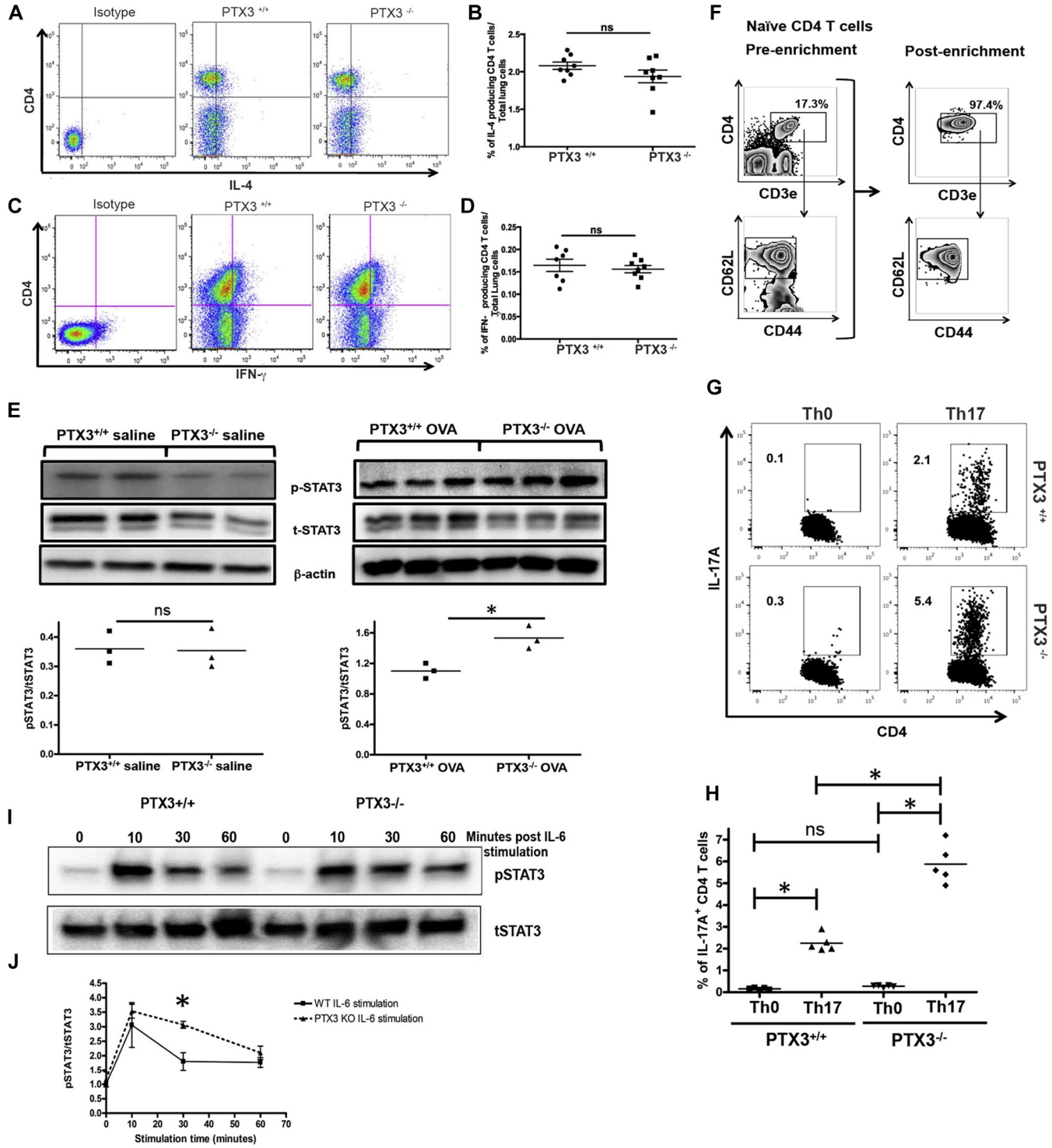

FIG E3. A-D, Flow cytometric analysis of expression profile of IL-4 (Fig E3, *A* and *B*), and IFN-γ (Fig E3, *C* and *D*) in lung CD4 T cells from OVA-exposed *Ptx3*$^{+/+}$ and *Ptx3*$^{-/-}$ mice. **E,** STAT3 phosphorylation was assessed by means of Western blotting in lungs of naive and OVA-exposed *Ptx3*$^{+/+}$ and *Ptx3*$^{-/-}$ mice (n = 3). **F,** Naive CD4 T cells were enriched from splenocytes and cultured in the presence of T_H17 polarization cocktail for 5 days. **G** and **H,** IL-17A–producing CD4 T cells after T_H17 polarization were assessed by means of flow cytometry. Quantification and statistical analysis of fluorescence-activated cell sorting data is shown as graphs (n = 5-6 per group). *$P < .01$. **I** and **J,** CD4 T cells were stimulated with 20 ng/mL IL-6, and STAT3 phosphorylation was detected by mean of Western blotting. The graph shows averages from 3 independent experiments. *$P < .01$. *ns,* Not significant.

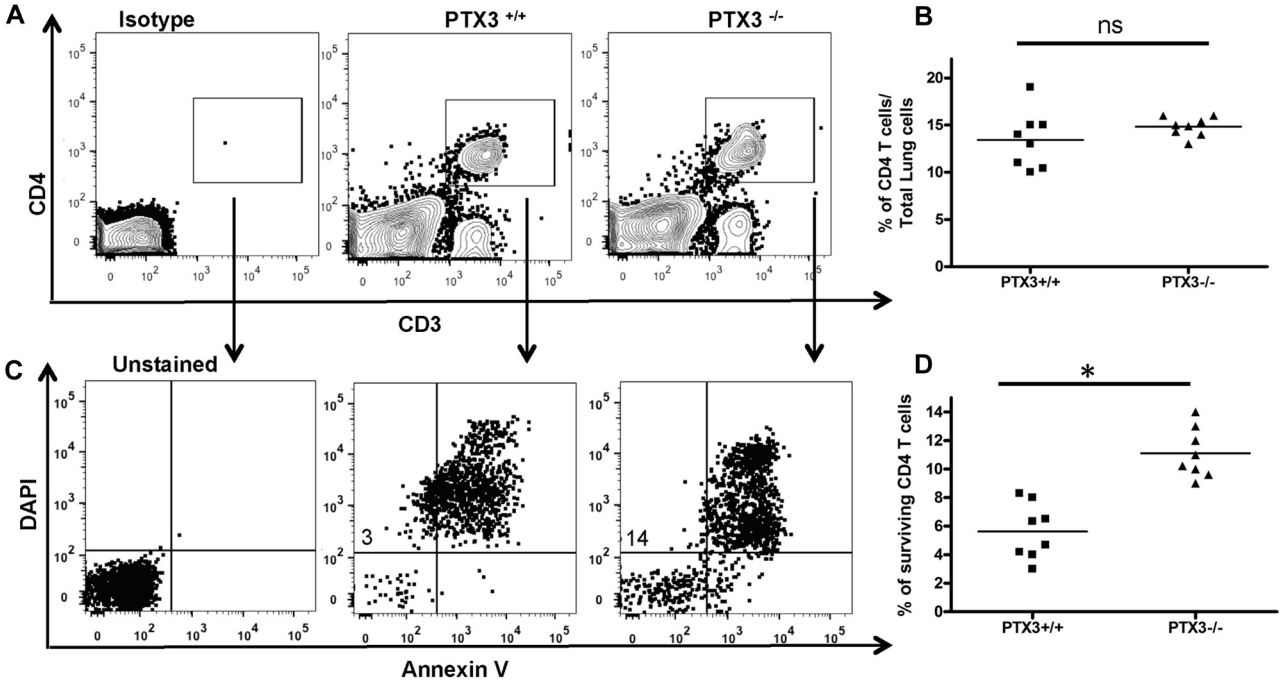

FIG E4. Naive lung CD4 T cells from *Ptx3*$^{+/+}$ and *Ptx3* $^{-/-}$ mice were cultured for 3 days (**A** and **B**), and survival of CD4 T cells was assessed by using Annexin V and 4′-6-diamisino-2-phenylindole dihydrochloride *(DAPI)* staining (**C** and **D**; n = 8 per group). *$P < .01$.

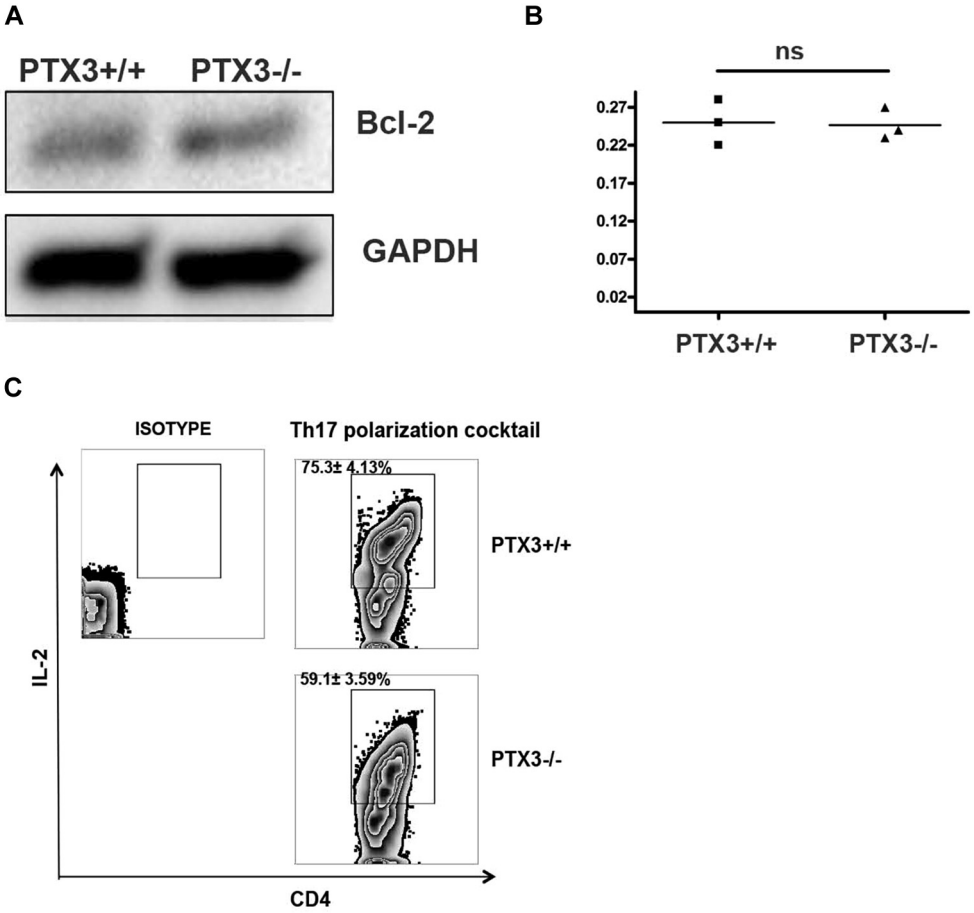

FIG E5. **A** and **B,** Bcl-2 expression was detected in naive CD4 T cells from *Ptx3*$^{+/+}$ and *Ptx3*$^{-/-}$ mice by using Western blotting (n = 3). **C,** Enriched naive CD4 T cells were cultured in the presence of T_H17 polarization cocktail for 5 days, and production of IL-2 by CD4 T cells from *Ptx3*$^{+/+}$ and P*tx3*$^{-/-}$ was assessed by means of flow cytometry (n = 5-6 per group). *ns*, Not significant.

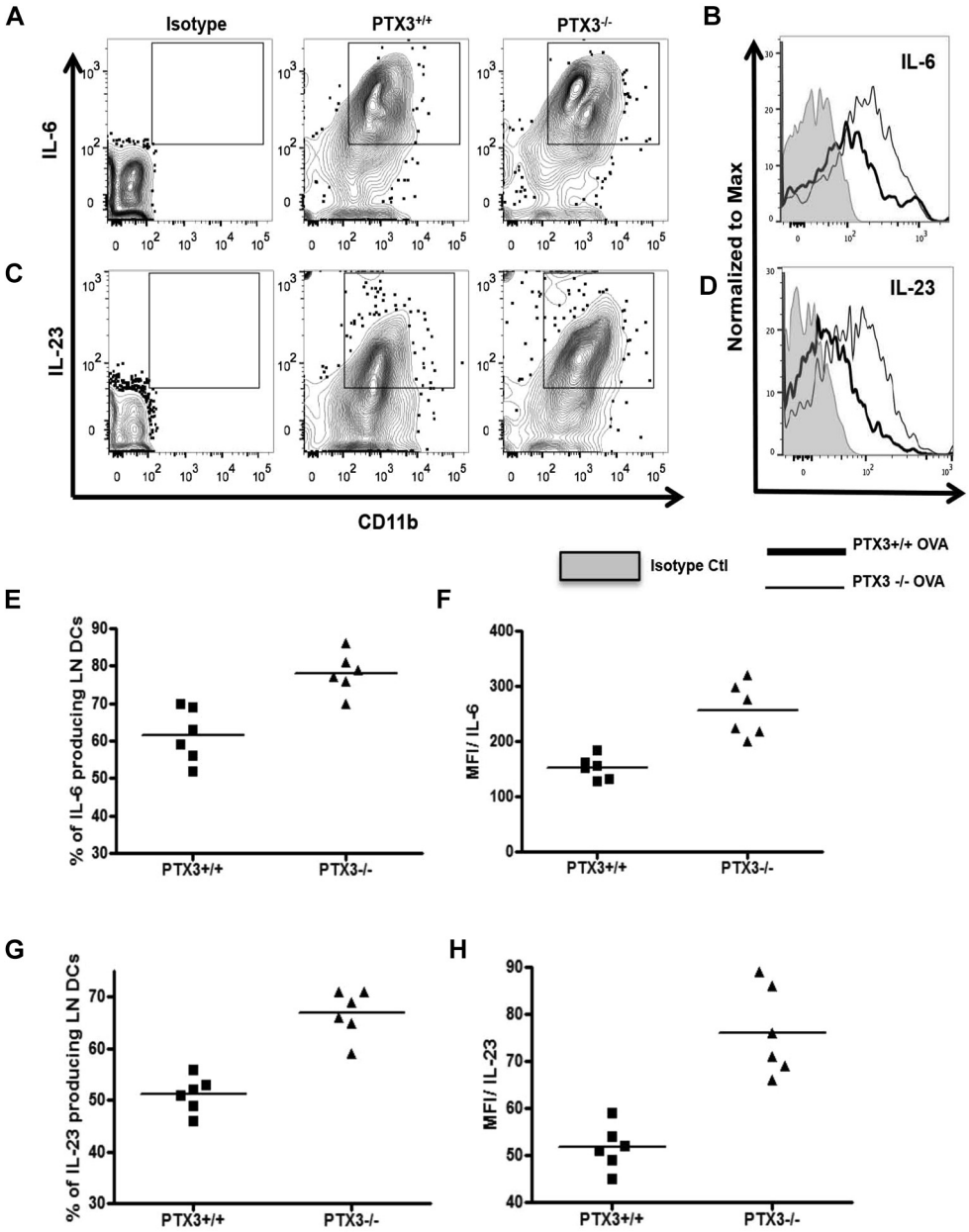

FIG E6. **A** and **B,** CD11c^{+}CD11b^{+} DCs from MLNs of OVA-sensitized/challenged *Ptx3*$^{+/+}$ and *Ptx3*$^{-/-}$ mice were assessed for intracellular IL-6 (**A** and **B**) and IL-23 (**C** and **D**) expression by using flow cytometry. The gating strategy is similar to that used in characterizing lung DCs (n = 6 per group). Quantitative analysis of IL-6 (**E** and **F**) and IL-23 (**G** and **H**) production is shown as graphs.

TABLE E1. Details of antibodies used for flow cytometry

Marker	Antibody clone	Company
CD3e	145-2C11	eBioscience
CD4	GK1.5	eBioscience
CD8	53-6.7	eBioscience
IL-17A	eBio17B7	eBioscience
IFN-γ	XMG1.2	eBioscience
CD69	N418	BioLegend
CD25	PC61	BioLegend
CD11b	M1/70	eBioscience
CD11c	N418	eBioscience
Gr-1	RB6-8C5	BioLegend
F4/80	BM8	eBioscience
IL-6	MP5-20F3	eBioscience
Siglec F	E50-2440	BD Biosciences
Bcl-2	BCL/10C4	BioLegend

TABLE E2. Details of primers used for mRNA analysis

Gene	Primer sequence
muc5ac	Reverse: 5′-GTT GCA GAG ACC AGG GAA GT3′
	Forward: 5′-GCA TGT TGG TAC CCC ACT CA 3′
muc5b	Reverse: 5′-CAG GTG TAA GGC GCT CAT GC 3′
	Forward: 5′-GAA ACT GGA GCT GGG CTC TG 3′
Gapdh	Reverse: 5′-ACA CAT TGG GGG TAG GAA CA 3′
	Forward: 5′-AAC TTT GGC ATT GTG GAA GG 3′
Il17a	Reverse: 5′-ACA CCC ACC AGC CAT CTT TC 3′
	Forward: 5′-TCC AGA AGG CCC TCA GAC TA 3′